PLOS GENETICS

RESEARCH ARTICLE

Notch pathway mutants do not equivalently perturb mouse embryonic retinal development

Bernadett Bosze[1], Julissa Suarez-Navarro[1], Illiana Cajias[1¤], Joseph A. Brzezinski IV[2], Nadean L. Brown[1]*

1 Department of Cell Biology & Human Anatomy, University of California, Davis, California, United States of America, **2** Department of Ophthalmology, University of Colorado Anschutz Medical Campus, Aurora, Colorado, United States of America

¤ Current address: Clinical Testing Lab, Marshall Medical Center, Placerville, California, United States of America
* nlbrown@ucdavis.edu

Citation: Bosze B, Suarez-Navarro J, Cajias I, Brzezinski IV JA, Brown NL (2023) Notch pathway mutants do not equivalently perturb mouse embryonic retinal development. PLoS Genet 19(9): e1010928. https://doi.org/10.1371/journal.pgen.1010928

Editor: Seth Blackshaw, Johns Hopkins University School of Medicine, UNITED STATES

Received: July 11, 2023

Accepted: August 16, 2023

Published: September 26, 2023

Peer Review History: PLOS recognizes the benefits of transparency in the peer review process; therefore, we enable the publication of all of the content of peer review and author responses alongside final, published articles. The editorial history of this article is available here: https://doi.org/10.1371/journal.pgen.1010928

Data Availability Statement: All relevant data are within the manuscript and its Supporting Information files.

Abstract

In the vertebrate eye, Notch ligands, receptors, and ternary complex components determine the destiny of retinal progenitor cells in part by regulating *Hes* effector gene activity. There are multiple paralogues for nearly every node in this pathway, which results in numerous instances of redundancy and compensation during development. To dissect such complexity at the earliest stages of eye development, we used seven germline or conditional mutant mice and two spatiotemporally distinct Cre drivers. We perturbed the Notch ternary complex and multiple *Hes* genes to understand if Notch regulates optic stalk/nerve head development; and to test intracellular pathway components for their Notch-dependent versus -independent roles during retinal ganglion cell and cone photoreceptor competence and fate acquisition. We confirmed that disrupting Notch signaling universally blocks progenitor cell growth, but delineated specific pathway components that can act independently, such as sustained Hes1 expression in the optic stalk/nerve head. In retinal progenitor cells, we found that among the genes tested, they do not uniformly suppress retinal ganglion cell or cone differentiation; which is not due differences in developmental timing. We discovered that shifts in the earliest cell fates correlate with expression changes for the early photoreceptor factor Otx2, but not with Atoh7, a factor required for retinal ganglion cell formation. During photoreceptor genesis we also better defined multiple and simultaneous activities for *Rbpj* and *Hes1* and identify redundant activities that occur downstream of Notch. Given its unique roles at the retina-optic stalk boundary and cone photoreceptor genesis, our data suggest Hes1 as a hub where Notch-dependent and -independent inputs converge.

Author summary

A long-standing question in biology is how cells respond to multiple signaling inputs with a specific response. Here we directly compared the genetic requirements of multiple genes

Funding: This work is supported by NIH, National cEye Institute (NEI) to NLB, R01-EY013612; NIH, National Eye Institute to NLB, R01-EY031724; NIH, National Eye Institute to JAB, R01-EY024272. Additional support from NIH P30 EY012576 grant, awarded to University of California, Davis.

Competing interests: The authors have declared that no competing interests exist.

in the Notch signaling pathway. These genes are components of a molecular cascade in responding cells that is triggered by Notch receptors binding to ligands on an adjacent cell. Notch signaling is an important regulator of retinal neuron formation, which acts in the presence of other signals. This results in multiple pathways converging on key, shared downstream target genes. Here we genetically removed four different Notch pathway genes during mouse embryonic eye development, either alone or in combinations, and analyzed the consequences. We found three situations, during tissue specification and retinal neurogenesis where the activities of these genes have both Notch-dependent and Notch-independent activities. Our data significantly extend current models of how the retina distinguishes itself from other tissues and how retinal progenitor cells decide to stop dividing and select particular neuronal fates. These findings extend current models regarding integration or branchpoints for signaling cascades.

Introduction

The central eye field in vertebrate embryos is specified at the end of gastrulation and splits to form bilateral optic vesicles that evaginate from the ventral diencephalon. Multiple signaling pathways regionalize and pattern the growing optic vesicles, demarcating the optic stalk (OS), optic cup (OC) and retinal pigment epithelium (RPE) tissues. The OC gives rise to the neural retina, which is an excellent system for studying cell fate specification and differentiation. The retina is comprised of seven major cell classes that arise in a tightly controlled, but overlapping chronological order: retinal ganglion cells (RGCs), cone photoreceptors, horizontals, and a subset of amacrine neurons—before birth; and amacrines, rods, bipolars and Müller glia—mainly after birth. These cell types are derived from proliferative multipotent retinal progenitor cells (RPC) that permanently stop diving before differentiating into neurons and glia. Throughout development, RPC pool size must be balanced with neuron and glia production to generate a functional retina [reviewed in 1,2].

The highly conserved Delta-Notch signaling pathway maintains the equilibrium between proliferation and differentiation in a myriad of tissues and often acts reiteratively within a single organ [3,4]. In brief, signaling starts at the cell membrane upon ligand-receptor binding, which induces sequential proteolytic cleavages of the Notch receptor and ultimately releases the Notch intracellular domain (N-ICD). N-ICD forms a ternary complex with Rbpj (Recombination signaling binding protein, also termed CBF1) and Maml (Mastermind-like) [4]. These ternary complexes bind DNA to transcriptionally activate target genes, including *Drosophila* ***H****airy* or ***E*** ***(****s****pl)***, and vertebrate *Hes* gene families [5–7]. In several tissues, the loss of canonical Notch signaling results in precocious flawed neurogenesis, whereas too much signaling induces overproliferation [8–21]. Therefore, the Notch pathway controls the balance between proliferation and differentiation during retinal development. Throughout development, naive RPCs progress through a transitional state, exit mitosis, commit to a fate, and differentiate [reviewed in 22]. Transitional RPCs downregulate the Notch reception machinery, but upregulate Notch ligands, presumably to communicate with nearby, naive RPCs [23–25]. Transitional RPCs also turn on competence factors that are necessary for neuronal fate choice, such as *Atoh7* for RGCs [26–31], and *Otx2* for photoreceptors [32–34]. The mechanisms for how competence factors steer cells to distinct cell fates, and their dependence on Notch signaling, remain unresolved.

Most vertebrate *Hes* genes are Notch ternary complex targets [7,35–38]. *Hes1*, *3* and *5* are important in the nervous system, whereas *Hes2*, *4* and *7* act in other parts of the body [7,39]. The role of *Hes6* in development is debatable [reviewed in 7]. Both *Hes1* and *Hes5* can exhibit oscillating expression patterns within stem cells or neural progenitors poised between

proliferation and differentiation [39]. For example, actively proliferating progenitor cells show high, oscillating *Hes1* levels, whereas low *Hes1* correlates with differentiation [40]. In the mouse spinal cord, *Hes5* can be either sustained or oscillatory, with its frequency of oscillation correlating with onset of differentiation [41]. *Hes1* is an essential gene, whose loss causes prenatal lethality along with embryonic morphogenesis defects characterized by premature differentiation [42]. By comparison, complete loss of *Hes3* and/or *Hes5* has no impact on viability, but can induce discrete defects, suggesting specific contexts when these paralogues are compensated by or redundant with *Hes1*. This is further supported by the increased severity of *Hes1;Hes3;Hes5* triple mutants in other parts of the central nervous system (CNS) [43–48]. Despite the importance of the Notch pathway in retinal neurogenesis, no functions have been reported for it during mammalian optic vesicle/cup outgrowth, patterning or morphogenesis. Moreover, *Hes* gene redundancy and compensation have not been explored in the developing retina or adjacent tissues. In the E13.5 mouse eye, both *Hes1* expression modes are present. RPCs oscillate while adjacent ONH/OS cells exhibit sustained *Hes1* expression [49,50]. As a Notch ternary complex target, removing *Hes1* is predicted to universally release the block on neuron differentiation, but paradoxically *Hes1* retinal mutants simultaneously have excess RGC neurons, but too few cone photoreceptors [14,42,50,51] (S1 Table). This implies the *Hes1* gene is where Notch-independent [52] and Notch-dependent regulation converge, with the latter complicated by *Hes* gene redundancy or compensation.

To understand the complexity of *Hes* gene function during development, we directly compared the embryonic eye phenotypes of *Hes* single versus multiple mutant mice [43,53]. Because *Hes* triple germline mutants die soon after gastrulation, a *Hes1* conditional mutation ($Hes1^{CKO/CKO}$) was combined with $Hes3^{-/-}$;$Hes5^{-/-}$ germline mutant alleles, to effectively generate tissue-specific *Hes* triple mutants (Hes^{TKO}) [43,53]. Importantly, we also asked how well Hes^{TKO} phenotypes match the rest of the Notch pathway by evaluating $Rbpj^{CKO/CKO}$ and $ROSA^{dnMaml\text{-}GFP/+}$ retinal mutants. The $ROSA^{dnMaml\text{-}GFP/+}$ allele is under flox-stop control, and dominantly creates inactive Notch transcriptional complexes, using a truncated Mastermind-nGFP fusion protein that binds with endogenous N-ICD and Rbpj [54–57]. For this study we used two Cre drivers (Rax-Cre and Chx10-Cre) with spatially overlapping, but temporally offset Cre activation, to tease apart morphologic versus neurogenic roles for each gene [50,58]. These experiments facilitated a direct phenotypic comparison among the allelic series, and integration of our findings with those from previous studies (S1 Table) [8–17].

Our direct comparisons of Hes^{TKO} versus *Rbpj* conditional mutants support that *Hes* genes regulate the balance between RPC growth and neurogenesis progression. We also discovered that Maml cofactor activities are not exclusive to the Notch ternary complex, in that $ROSA^{dnMaml\text{-}GFP/+}$ retinal mutants have unique nasal-temporal patterning defects. We determined that sustained Hes1 expression is Notch-independent, whereas in the retinal compartment, *Hes1* and *Hes5* are partially redundant downstream of Notch. Our phenotypic analyses of early neurogenesis reveal both Notch-dependent and -independent functions that influence RPC progression into early competence states, and further highlight directly opposing roles for *Rbpj* and *Hes1* regarding cone fate. Although Hes^{TKO} mutants partially rescue the *Hes1* cone phenotype, they do not fully recapitulate those of *Notch1* or *Rbpj* mutants [10,14,16,17]. We conclude that unknown genetic inputs, independent from Notch signaling, also impact early neurogenesis and act via competence factors to affect RGC and cone photoreceptor fate determination.

Results

During mouse nervous system development, *Hes1* appears in the anterior neural plate, optic vesicle and optic cup several days prior to the onset of retinal neurogenesis [42,59]. We first

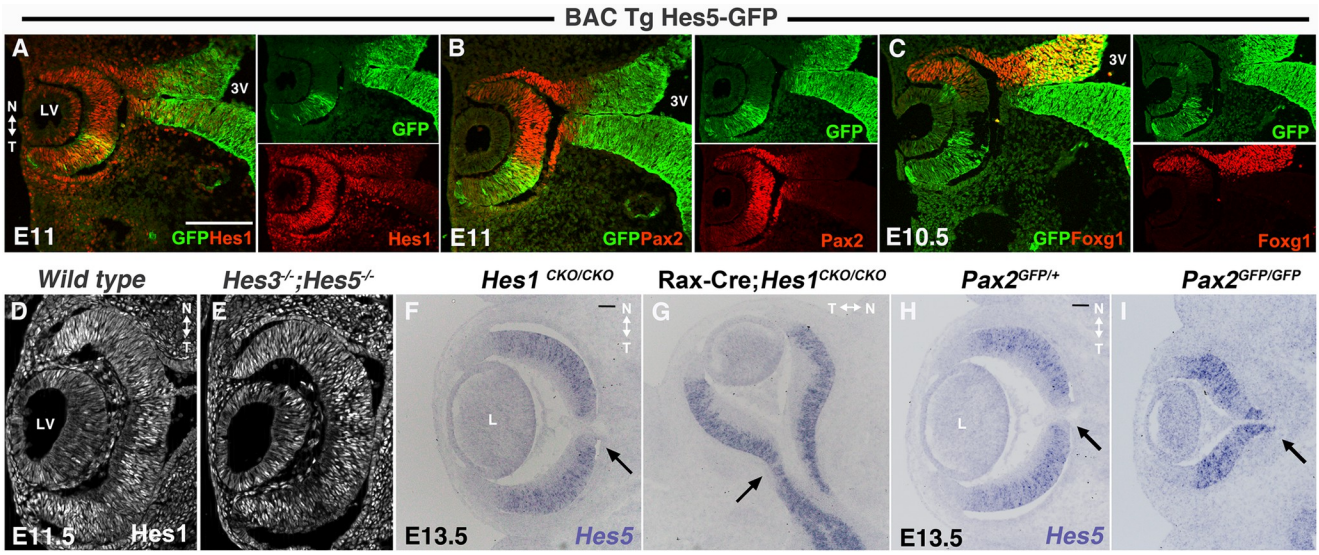

Fig 1. *Hes* genes in the embryonic mouse eye. (A) Hes1 and Hes5-GFP colabeling at E11.0 shows uniform Hes1 expression, and BAC Tg(*Hes5*-GFP) expression in the temporal optic cup and most of the optic stalk and adjacent diencephalon. (B) At this stage, Pax2 and Hes5-GFP are largely mutually exclusive, with Pax2 expression transiting from uniform to ONH/OS domain restriction [65]. OS and brain progenitors surrounding the third ventricle (3V) have not yet differentiated. (C) At E10.5 Hes5-GFP and Foxg1 are not coexpressed in the optic cup, as they are in the nasal brain (yellow domain). (D, E) By E11.5, Hes1 now exhibits oscillating optic cup expression, which is unaffected in *Hes3*$^{-/-}$;*Hes5*$^{-/-}$ double mutants. (F-G) At E13.5 *Hes5* mRNA expression is inappropriately expanded in the retinal territory that invaded the OS (arrows), after Rax-Cre removal of *Hes1*(G); Chx10-Cre-induced *Hes1* mutants have normal *Hes5* expression (S2 Fig). (H-I) *Hes5* mRNA similarly expands in *Pax2*$^{GFP/GFP}$ mutants with retina-ONH boundary (arrows) defects [65]. N = nasal; T = temporal; LV = lens vesicle; L = lens; 3V = third ventricle; Bar in A = 10 microns, in F,H = 100 microns; n ≥3 per age and genotype.

https://doi.org/10.1371/journal.pgen.1010928.g001

compared the expression of multiple *Hes* genes throughout embryonic eye development (Fig 1). At these early stages, *Hes1* mRNA and protein are uniformly expressed (Fig 1A). As the first cohort of retinal progenitor cells (RPCs) cells exit mitosis and differentiate into neurons, there is a switch in Hes1 expression to a "salt-n-pepper" pattern within mitotic RPCs (Fig 1D). However, optic nerve head (ONH) and optic stalk (OS) cells retain uniform Hes1 expression [50] (also see Fig 2A). By contrast, *Hes5* mRNA appears later within RPCs just ahead of the first neurons [60]. The mouse Hes5-GFP BAC transgene is an accurate reporter of *Hes5* expression, enabling direct correlation with Hes1 and other markers during development [60]. Hes5-GFP is also found in the diencephalon (Fig 1A–1C), but not in optic stalk cells that express Pax2 (Fig 1B). At E11, there are no Hes5-GFP+ cells in the nasal optic cup as marked by Pax2 and Foxg1 (Fig 1B and 1C). *Hes3* functionally overlaps with *Hes1* in the brain isthmus and is active in the CNS as early as E9.5 [61]. Nonetheless, we did not detect *Hes3* mRNA in the retina prior to E18 [62]. We conclude that *Hes1* is activated well before *Hes5*, which turns on in a subset of RPCs just prior to the onset of neurogenesis. *Hes1* is expressed in distinct modes, appearing to oscillate in RPCs while exhibiting a high sustained level in the optic stalk.

Next, we asked whether Hes1 depends on other *Hes* genes. *Hes3* and *Hes5* are <1Mb apart on mouse chromosome 4, and their knockout alleles are transmitted together as one mutant haplotype (S2 Table) [43,49]. We confirmed that *Hes3*$^{-/-}$;*Hes5*$^{-/-}$ mutants have normal retinal morphology and cell-type composition across eight developmental stages (E10.5-P21) (S1 Fig). We examined Hes1 ocular expression from E10.5-E16.5 within *Hes3*$^{-/-}$;*Hes5*$^{-/-}$ mice, and found that both oscillating RPC and sustained ONH/OS Hes1 domains were normal (Figs 1D,1E and 2C). Thus, *Hes1* is not cross-regulated by either *Hes3* or *Hes5*. Then, we checked for reciprocal regulation by evaluating *Hes5* mRNA in E13.5 and E16.5 *Hes1* conditional (CKO) mutants, using two Cre drivers whose activation is temporally offset. Rax-Cre initiates recombination as

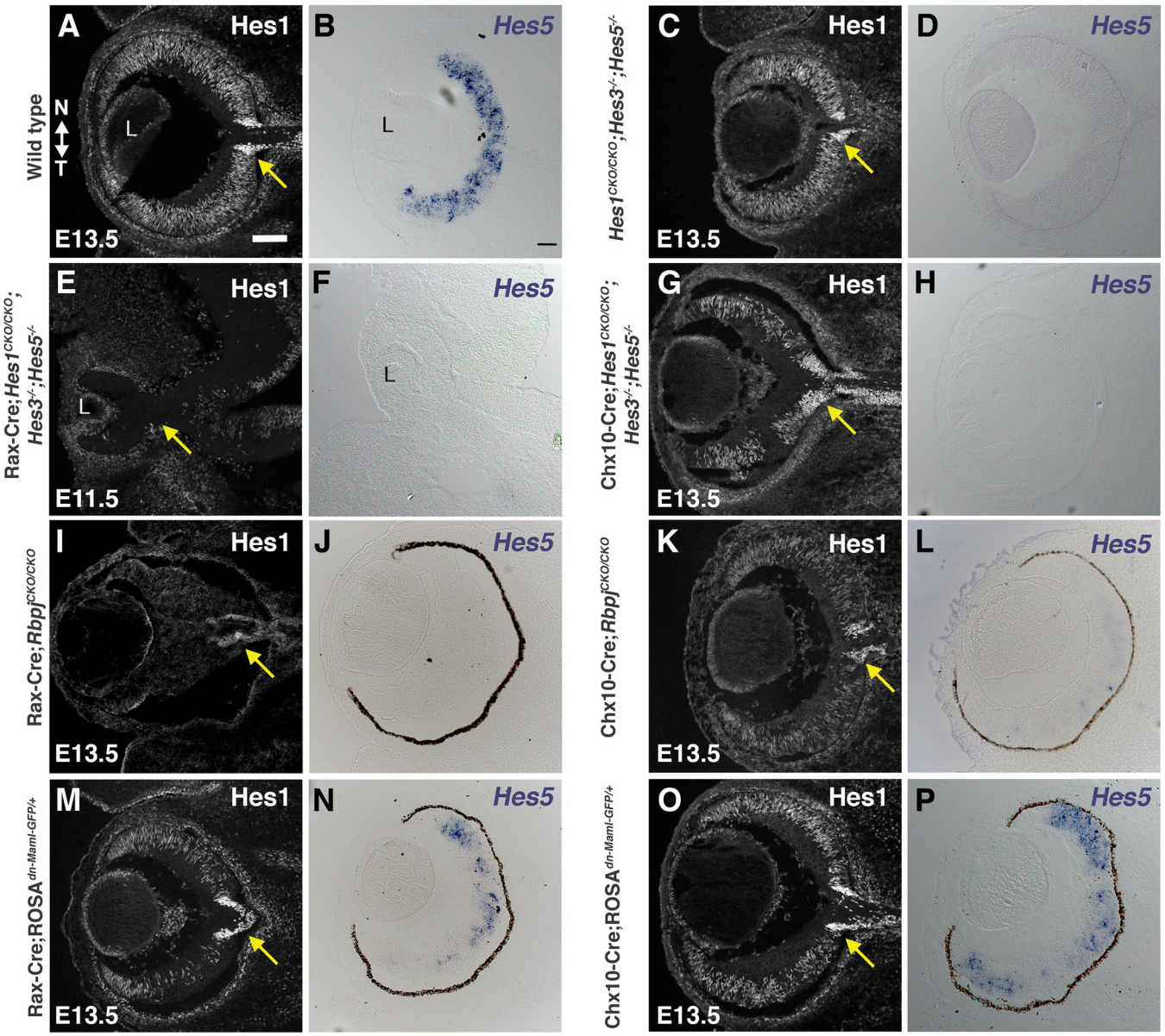

Fig 2. *Hes1* and *Hes5* expression in *Rbpj*, dnMAML and *Hes* triple retinal mutants. (A,C,E,G,I,K,M,O) Anti-Hes1 labeling of E11.5 or E13.5 cryosections. Hes1 is missing in Rax-Cre;Hes^{TKO} and Rax-Cre;$Rbpj^{CKO/CKO}$ RPCs (E, I), with the intense Hes1+ ONH domain (yellow arrows) only lost in Rax-Cre;Hes^{TKO} eyes. (B,D,F,H,J,L,N,P) *Hes5* mRNA is missing in all *Hes5* germline mutants. Both *Rbpj* conditional mutants effectively block *Hes5* mRNA expression (J,L). dnMAML partially knocks down Hes1 (M,O) and *Hes5* (N,P). The effect is stronger in Rax-Cre;$ROSA^{dnMaml1\text{-}GFP/+}$ eyes, but both conditions showing a more pronounced effect in the temporal optic cup. All panels oriented nasal up and temporal down (noted in A), with L = lens in A,B,E,F; scalebar in A = 100 microns, B = 50 microns; n = 3/3 mutants per genotype.

https://doi.org/10.1371/journal.pgen.1010928.g002

early as E8.5 and acts in the ventral thalamus/hypothalamus, optic vesicle, cup and stalk, RPE, ONH and RPCs. The Chx10-Cre driver deletes genes from E10.5 onwards, exclusively in RPCs [50,58,63]. Upon earlier and broader deletion using Rax-Cre, *Hes5* mRNA abnormally extends into the E13.5 optic stalk (Fig 1G), whereas *Hes5* mRNA was unaffected in later-deleting Chx10-Cre;$Hes1^{CKO/CKO}$ mutant retinas (S2 Fig). Previous studies suggested that Hes1 can suppress *Hes5* in the developing CNS [46,60,64]. However, expansion of the *Hes5* mRNA domain in Rax-Cre;$Hes1^{CKO/CKO}$ retinas could be coincident with ectopic retinal tissue

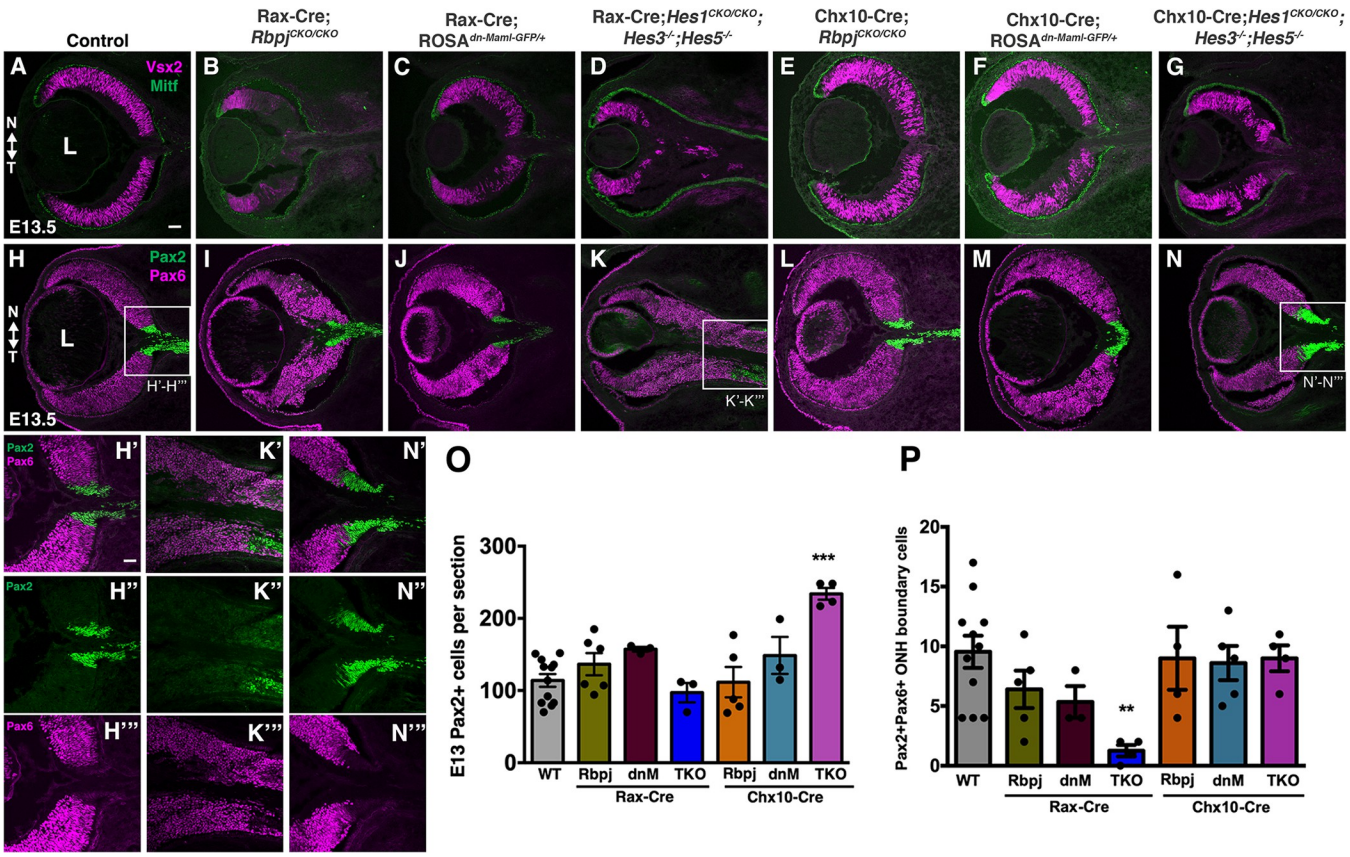

Fig 3. Ocular tissue patterning defects among Notch pathway mutants. (A-G) Vsx2 and Mitf double labeling marks E13.5 RPCs (fuchsia) and RPE cells (green), respectively. Vsx2+ RPCs were disorganized in the all mutants, with this domain displaced in Rax-Cre;*Rbpj*$^{CKO/CKO}$ and Rax-Cre;*Hes*^{TKO} eyes (B,D). (H-N) Pax6-Pax2 colabeling delineates the retinal-optic stalk boundary, with boxed regions in H,K,N shown at higher magnification in H' to N'''. (O) Quantification of total Pax2+ cells per section (P) Quantification of Pax6+Pax2+ cells per section at retinal-ONH interface (both boundaries). Graphs display individual replicate data points, the mean and S.E.M; Significant Welch's ANOVA, plus pairwise comparisons to wild type (***p<0.001, **p<0.01). Rax-Cre; *Hes*^{TKO} eyes have a more elongated Pax6 domain (K, K'-K''') with no impact on the size of the Pax2+ domain (O), but a significant loss of double-labeled boundary cells (P). Only Chx10-Cre;*Hes*^{TKO} eyes had an enlarged Pax2 domain (N, N'-N''';O). All panels oriented nasal up (noted in A, H), L = lens in A,H; scalebar = 50 microns in A, 100 microns in H'; n $\geq$ 3 biologic replicates/genotype.

https://doi.org/10.1371/journal.pgen.1010928.g003

formation in this mutant [38]. To distinguish between these possibilities, we assayed *Hes5* expression in *Pax2*$^{GFP/GFP}$ (germline) mutants, which also have ectopic retinal tissue in the optic stalk [65,66]. Here too, we found the *Hes5* mRNA domain was inappropriately expanded (Fig 1I). Thus, we conclude that ectopic retina formation, rather than *Hes1* suppression of *Hes5*, is the cause of expanded *Hes5* in our Rax-Cre;*Hes1*$^{CKO/CKO}$ mutants.

The loss of multiple *Hes* genes is more catastrophic than loss of *Hes1* alone in several regions of the embryo [reviewed in 7]. We used the two Cre drivers with *Hes*^{TKO} mice (*Hes1*$^{CKO/CKO}$; *Hes3*$^{-/-}$;*Hes5*$^{-/-}$) to test this idea in the optic cup and stalk. We collected litters at E11, E13.5, E16.5, P0 (birth) (S2 Table). Rax-Cre;*Hes*^{TKO} mutants were not viable beyond E13, but displayed more severe phenotypes than *Hes1* single mutants (S2 Table, Figs 3 and 4) [50]. For the surviving Chx10-Cre;*Hes*^{TKO} mice, we directly compared their P21 ocular phenotypes to Chx10-Cre;*Hes1*$^{CKO/CKO}$ single mutants (S3 Fig). *Hes1* single mutants had defective retinal lamination, rosettes, and occasionally a small, vitreal cell mass (S3B Fig boxed area). By contrast, adult Chx10-Cre;*Hes*^{TKO} eyes had more severe retinal lamination and rosetting defects and conspicuous microphthalmia (S3C and S3D Fig). In some sections, ectopic tissue in the vitreous appeared contiguous with the ONH (S3C and S3D Fig boxed areas). We performed

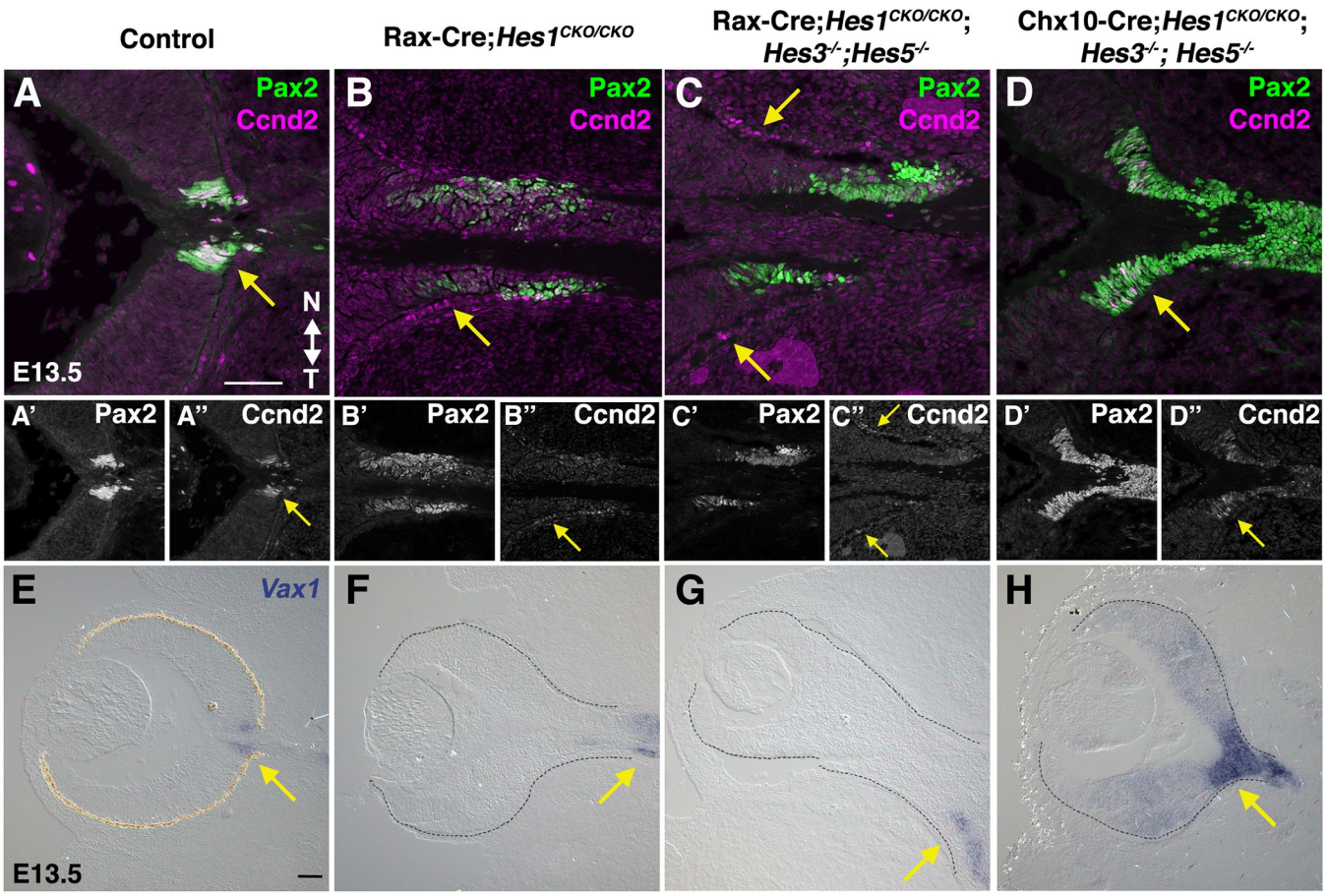

Fig 4. *Hes1 and Hes*^{TKO} retina-ONH boundary phenotypes. (A-D") Pax2 and Ccnd2 immunolabeling at E13.5. Normally, Pax2 and Ccnd2 are coexpressed in ONH cells. In Rax-Cre;*Hes1*$^{CKO/CKO}$ and Rax-Cre;*Hes*^{TKO} eyes, the Pax2 OS domain is elongated, with Ccnd2 expression dramatically downregulated in the optic stalk or mislocalized into the RPE (arrows in A,A", B,B",C,C"). Intriguingly, in Chx10-Cre;*Hes*^{TKO} eyes, both Pax2 and Ccnd2 domains expanded into the optic cup (arrows in D, D"). (E-H) *Vax1* mRNA expression in the ONH/OS (arrows). Eyes in F-H are albino and the retina is outlined with dotted lines. The *Vax1* domain shifted toward the brain in Rax-Cre;*Hes1*$^{CKO/CKO}$ and Rax-Cre;*Hes*^{TKO} eyes, but in Chx10-Cre;*Hes*^{TKO} eyes it was expanded both into the retina and towards the brain. All panels oriented nasal up (noted in A) and the diencephalon to the right; n = 3 biologic replicates/genotype.

https://doi.org/10.1371/journal.pgen.1010928.g004

Tubb3/Endomucin (Emcn) colabeling of the ectopic tissue to assay for neurons and blood vessels, respectively (S3E–S3L' Fig). Although blood vessels (Emcn+ cell membranes, pink arrows) and autofluorescent red blood cells (asterisks) were obvious, Tubb3+ neurons were difficult to observe, suggesting this ectopic tissue may have a nonneuronal origin. Overall, we observed that *Hes*^{TKO} mutants are more severe than single *Hes1* mutants or *Hes3/5* double mutants. Our findings argue that *Hes* genes act in a complex, yet incompletely redundant fashion during eye development. To unravel this complexity, we initiated a deeper phenotypic evaluation at E13.5, when Rax-Cre triple mutants are viable and the ONH is fully formed.

Hes^{TKO} and *Rbpj* mutants are the most severe

In theory, combined *Hes* functions should reflect those of the Notch ternary complex, which transcriptionally activates *Hes* genes. So we asked to what extent *Hes*^{TKO} ocular mutants phenocopy the loss of ternary complex gene function. This also allowed us to bypass complexity at the receptor level, as three Notch receptors are expressed in the prenatal mouse eye [11,67]. We opted to directly compare conditional mutant phenotypes for *Rbpj* and *dnMAML*

(dominant allele that creates inactive Notch transcriptional complexes) to those for Hes^{TKO}, using the same Cre drivers (Fig 2). In E11.5 Rax-Cre;Hes^{TKO} eyes, RPC and ONH/OS cells are devoid of Hes1 protein and *Hes5* mRNA as expected (Fig 2E). Because Chx10-Cre activates later and only within the retina [50], we expected there would be a loss of Hes1 from RPCs, but not ONH/OS cells. However, in E13.5 Chx10-Cre;Hes^{TKO} eyes, Hes1 clearly persists in both domains (compare Fig 2A and 2G). Since Hes1 is spotty in the retina and dependent upon Cre mediated recombination, we hypothesized this its pattern is due to mosaic Chx10-Cre expression [58,68]. This is further supported by immunostaining for Rbpj in Rax-Cre versus Chx10-Cre $Rbpj^{CKO/CKO}$ mutants (S4 Fig). Moreover, we observed that E13.5 Rax-Cre;$Rbpj^{CKO/CKO}$ mutants had a cell autonomous loss of Rbpj from RPC, ONH/OS, and RPE cells as expected (compare S4A, S4B and S4B' Fig). Although Hes1 was absent from the optic cup and RPE (compare S4A' and S4B" Fig), ONH/OS cells still express Hes1. Thus, we conclude sustained Hes1 expression in the ONH/OS is independent of Notch, whereas its expression in the retina depends upon Rbpj and Notch signaling.

We took advantage of a Cre-GFP fusion protein within the Chx10-Cre driver to directly compare GFP and Rbpj coexpression in Chx10-Cre;$Rbpj^{CKO/CKO}$ and control Chx10-Cre; $Rbpj^{CKO/+}$ retinal sections (S4C, S4E, S4G and S4I Fig). This Chx10-Cre BAC transgene encodes a Cre-GFP fusion protein, allowing us to test cell autonomy in the GFP+ cell population [58]. At E13.5 we noted a strong autonomous knockdown of Rbpj protein (S4C" Fig vs S4E" Fig), yet at E16.5 there were more Rbpj-expressing retinal cells that lacked GFP, identifying them as wild type (compare S4G' Fig to S4I' Fig). Hes1 was partially autonomously downregulated at both ages, mirroring what was seen with Rbpj (S4D, S4F, S4H, S4J Fig). Thus, we concluded that Chx10-Cre phenotypes generated through E13.5 are informative, but beyond this stage the wild type cohort (GFP-neg) outcompetes mutant (GFP+) cells [69,70], providing ample levels of Notch signaling and partially rescuing development. Evaluation of *Hes5* mRNA further confirmed Rax-Cre as the more effective driver, since we could still detect *Hes5* in Chx10-Cre;$Rbpj^{CKO/CKO}$ retinas (compare Fig 2J to Fig 2L). So, subsequent analyses were confined to E13.5, when Rax-Cre mutants are viable and Chx10-Cre mosaicism is less impactful. Next, we examined *Hes1* and *Hes5* expression in E13.5 Rax-Cre;$ROSA^{dnMAML\text{-}GFP/+}$ and Chx10-Cre;$ROSA^{dnMAML\text{-}GFP/+}$ retinas. Hes1 and *Hes5* are only modestly reduced, with a stronger effect seen in the temporal retina (Fig 2M–2P). There was a stronger knockdown in the Rax-Cre;$ROSA^{dnMAML\text{-}GFP/+}$ retinas (Fig 2M–2P). In neither case did we observe a loss of Hes1 in the ONH/OS area, further suggesting that it is independent of Notch signaling. The moderate phenotypes we observed did not fit our expectation that dnMAML misexpression would closely match the loss of *Rbpj*. Thus, we presume this *dnMAML* allele exhibits only a partial dominant negative effect in the developing eye. We decided to analyze this allele further to learn when, where and the degree to which it mimics $Rbpj^{CKO/CKO}$ and Hes^{TKO} mutants.

Notch signaling has no impact optic cup patterning

The optic vesicle and cup are patterned along dorsal-ventral (D/V) and nasal-temporal (N/T) axes. *Hes1* mutants have no D/V ocular phenotypes [50,59]. We checked for mispatterning of the N/T axis, since the Pax2 domain is displaced in Rax-Cre; $Hes1^{CKO/CKO}$ eyes, and *Pax2* germline mutants have abnormal N/T ocular patterning [65]. We compared the nasal-restricted marker Foxg1 [71,72] among the six Rax-Cre or Chx10-Cre-induced mutants at E13.5 and E16.5 (S5 Fig). We noted normal Foxg1 retinal expression, with two exceptions. At E13.5 Rax-Cre;Hes^{TKO} eyes, the Foxg1 nasal retinal domain was contiguous with the nasal optic stalk (S5D Fig). This is reminiscent of younger stages (Fig 1C), since at E13.5 Foxg1 in the wild type condition is no longer made in the nasal OS domain (S5A Fig). Based on RPC

domain expansion into the optic stalk (Fig 1G, see below), we conclude that this change in Foxg1 expression is another indication that the retina has expanded. The other exception is in E16.5 Rax-Cre;*ROSA*$^{dnMAML\text{-}GFP/+}$ mutants. In this case, Foxg1 was mislocalized to the temporal retina and subretinal space (arrow in S5J Fig), a cell-free zone between the apical retina and RPE. We presume these displaced cells are RPCs, since some Notch pathway mutants lose the outer limiting membrane along the apical side of the optic cup, allowing cells to spill into the subretinal space [73,74].

The optic cup splits into retina and RPE during or soon after DV/NT patterning of the retina. Vsx2/Chx10 (RPCs) and Mitf (RPE) transcription factors delineate these tissues, and actively maintain this boundary [75–77]. We compared Vsx2 and Mitf expression among all six E13.5 mutants (Fig 3A–3G), expecting a normal boundary, but that there would be fewer RPCs. All E13.5 Rax-Cre-generated mutants had noticeably smaller eyes (Fig 3B, 3C and 3D), but Chx10-Cre generated mutants were typically of normal size (Fig 3E–3G). For all six allelic combinations, the RPE formed correctly, but in Rax-Cre;*Hes*^{TKO} eyes this tissue extended into the optic stalk (Fig 3D), phenocopying Rax-Cre; *Hes1*$^{CKO/CKO}$ mutants [50]. Rax-Cre;*Rbpj*$^{CKO/CKO}$ and Rax-Cre;*Hes*^{TKO} mutants shared a RPC defect, namely patches of Vsx2-negative cells in the proximal optic cup, where neurogenesis normally initiates (Fig 3B–3D). Taken together, we conclude that Notch signaling has no overt role in D/V and N/T patterning, or retinal/RPE specification (Fig 3B).

Hes1 is Notch-independent at the optic cup-stalk boundary

At E12, the neural retina and optic stalk tissues become delineated, also establishing a ring of cells called the optic nerve head (ONH). ONH cells ultimately adopt glial fates and its interface with the retina is delineated by the generally abutting expression of the transcription factors Pax6 (RPCs) and Pax2 (ONH/OS) [66]. Although the molecular mechanisms regulating this boundary are not well understood, its formation requires both *Hes1* and *Pax2* activities [50,65,66]. To understand whether Notch signaling controls formation of this boundary, we performed Pax6/Pax2 colabeling at E13.5 among all mutants (Fig 3I–3N). The Rax-Cre;*Hes*^{TKO} eyes, were the most severe, with Pax6+ retinal tissue extending into the optic stalk territory, displacing the Pax2 domain (boxed area in Fig 3K). Although the Pax6-Pax2 boundary is intact in Rax-Cre;*Rbpj*$^{CKO/CKO}$ eyes, the shape of the ONH was attenuated compared to controls (Fig 3I). Interestingly, the proximal-most optic cup cells, those lacking Vsx2, still expressed Pax6 (compare Fig 3B to Fig 3I), suggesting these cells may have differentiated into neurons, since Pax6 is also expressed by nascent RGCs [69,78]. The Rax-Cre;*ROSA*$^{dnMAML\text{-}GFP/+}$ eyes were largely unaffected, but ONH shape was abnormal (Fig 3J). In all three Chx10-Cre generated mutants, a Pax6-Pax2 boundary was clearly discernable (Fig 3L–3N). But for Chx10-Cre; *Hes*^{TKO} mutants, Pax2 was uniquely ectopic within the retinal territory (box in Fig 3N), demonstrating overlapping *Hes* gene function at this boundary (Fig 3D, 3K and 3N). We quantified the total number of Pax2+ cells per section (Fig 3O) and the small number of Pax6-Pax2 coexpressing "boundary" cells (Fig 3P). These data confirmed that although displaced, the Pax2-expressing ONH is of typical size in Rax-Cre;*Hes*^{TKO} eyes (Fig 3K, 3K', 3K"–3O), and there was a significant loss of Pax6-Pax2 coexpressing boundary cells, most likely due to retinal extension (Pax6-only cell, Fig 3P). Moreover, only Chx10-Cre;*Hes*^{TKO} mutant eyes had an expanded Pax2 domain (Fig 3N, 3N'–3N" and 3O), but with normal boundary cell composition (Fig 3P).

The ONH and brain isthmus share multiple features, including Pax2 and sustained Hes1 expression [49,61,79], Brain isthmus cells have slower cell cycle dynamics than those in adjacent neural compartments with oscillatory expression [80]. Cyclin D2 (Ccnd2) is expressed by brain glial cells and intermediate neural progenitors with slow cycling kinetics [81,82] and

interestingly, E13.5 ONH cells normally express Ccnd2, which is regulated by Notch signaling in other ocular tissues [83,84]. We observed that Ccnd2 is downregulated in Rax-Cre;$Hes1^{CKO/CKO}$ and Rax-Cre;Hes^{TKO} mutants with mispositioned Pax2 domains (arrows in Fig 4B and 4C). Interestingly, Chx10-Cre;Hes^{TKO} eyes also downregulate Ccnd2 expression. Because *Hes1* encodes a transcriptional repressor, we presume its impact on Ccnd2 expression to be indirect. Once again, only Chx10-Cre;Hes^{TKO} retinal cells ectopically expressed Pax2 (Figs 3O and 4D), consistent with ONH expansion in $Pax2^{GFP/GFP}$ mutants [65]. Without *Pax2*, retinal cells are unable to lock-in a neural development program expressing both RPC and ONH markers [65]. This prompted us to ask whether Hes^{TKO} and *Pax2* mutants phenocopy one another regarding the mispatterning of the ONH/OS marker *Vax1* [85–87](Fig 4E–4H). In Rax-Cre;$Hes1^{CKO/CKO}$ and Rax-Cre;Hes^{TKO} eyes *Vax1* was shifted in the OS (arrows in Fig 4F–4G). But only in Chx10-Cre;Hes^{TKO} eyes had a *Vax1* domain that extended in the opposite direction, into the retina (Fig 4H). These data suggest that sustained *Hes1* in the ONH helps lock-in the boundary with the retina, whereas multiple *Hes* genes in adjacent RPCs are necessary for maintaining neurogenic potential.

Notch signaling regulates both RPC growth and death

Throughout the CNS, Notch signaling stimulates progenitor cell growth and blocks neurogenesis. Reduced RPC proliferation is common to all mutants in this pathway, although the magnitude of this loss is variable (S1 Table). We expected proliferation to be reduced in the six mutants and confirmed it by quantifying PhosphoHistone H3 (PH-H3) expression within G_2 and M-phase cells (Fig 5A–5G and 5O). Both *Rbpj* mutants have the fewest mitotic cells. There was also a modest loss of PH-H3+ cells in Hes^{TKO} mutants for the Chx10-Cre driver, but not Rax-Cre. The opposite outcome was seen in $ROSA^{dnMAML\text{-}GFP/+}$mutants. Thus, all six mutants do not equivalently lose PH-H3+ cells, which might be due to slight differences in the degree and age of phenotypic onset between Cre mouse lines.

In the E13-E16 retina, *Notch1*, *Rbpj* and *Hes1* mutants have a significant increase in apoptosis (S1 Table) [14,16,17,50]. We used cPARP labeling to quantify dying cells among the six mutants to determine if they were equivalent (Fig 5H–5N and 5P). We observed the anticipated increase in cPARP+ cells in E13.5 Rax-Cre;$Rbpj^{CKO/CKO}$ mutants (Fig 5I–5P), but all other genotypes were unaffected (Fig 5P). This suggests that Rax-Cre;Hes^{TKO} mutants can rescue the apoptosis phenotype previously described for *Hes1* single mutants [50]. This difference could be attributed to either *Hes1* and *Hes5* coordinated regulation of RPC target genes, or inherent interactions between retinal and ONH tissues, which impacts cell viability.

Notch pathway regulation of prenatal retinal cell fate

The loss of Notch signaling accelerates neurogenesis among a heterogeneous population of RPCs, allowing premature differentiation of multiple fates (e.g., RGC and photoreceptor). Previous work demonstrated that deletion of *Dll1*, *Dll4*, *Notch1*, or *Rbpj* induced ectopic differentiation of both RGCs and cone photoreceptors (S1 Table) [10,13–16]. Another archetypal defect of blocking Notch signaling is the appearance of retinal rosettes full of excess Crx+ photoreceptors (S1 Table). While *Hes1* conditional mutants also contain retinal rosettes, they uniquely *downregulate* Otx2, Crx, and cone photoreceptor markers, which cannot be attributed to developmental delay [14]. This incongruity raises questions about how the Notch pathway, downstream of the ternary complex, operates in transitional RPCs relative to competence factor expression and cell fate acquisition. We also reasoned that if Hes activities are partially redundant in transitional RPCs, the simultaneous removal of multiple *Hes* repressor genes might restore or even overproduce cones. To explore these ideas, we colabeled all six mutants

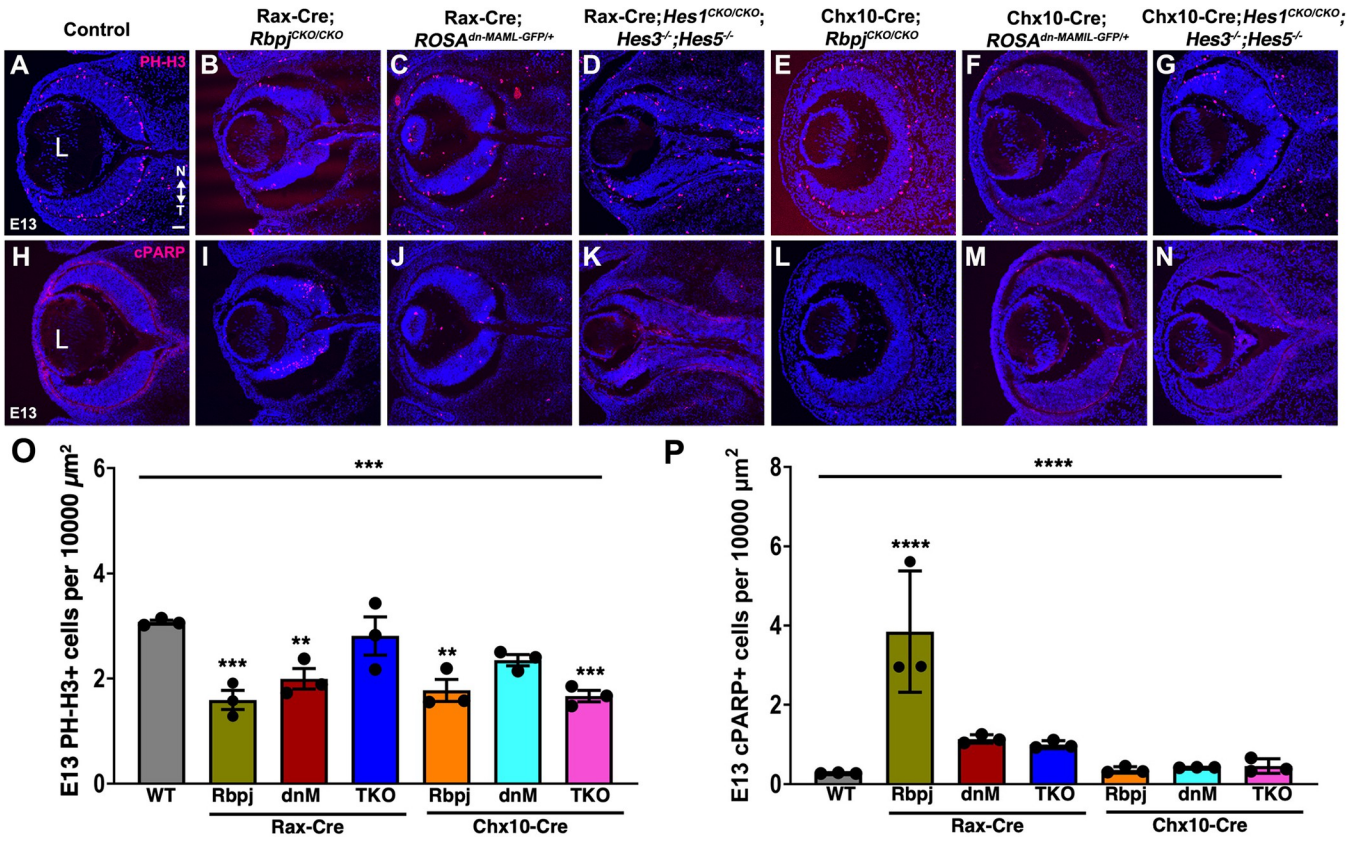

Fig 5. All E13.5 mutants have reduced proliferation, but only *Rbpj* mutants have excess apoptosis. (A-G) M-phase RPCs labeled with anti-PhosphoHistone-H3 (PH-H3) in red, DAPI in blue. (H-N) E13.5 cPARP+ apoptotic retinal cells in red, DAPI in blue. (O,P) Graphs display individual replicate data points normalized to optic cup area, the mean and S.E.M; Significant Welch's ANOVA, plus pairwise comparisons to wild type (****$p< 0.0001$, ***$p<0.001$, **$p<0.01$). All panels are oriented nasal up (noted in A), with L = lens; scalebar in A = 50 microns; n = ≥2 sections from 3 biological replicates/genotype.

https://doi.org/10.1371/journal.pgen.1010928.g005

at E13.5, for the competence factors Atoh7 and Otx2 [24,29,32,34,88](Fig 6A–6G), and labeled adjacent sections for the RGC-marker Rbpms [89,90] and photoreceptor marker Crx [34,89–95] (Fig 6H–6N). We also qualitatively assessed ectopic neurogenesis using the general neuronal marker Tubb3 (Fig 6O–6U).

Consistent with other studies, we noted defective retinal patterning at E13.5, with rosettes containing Otx2+ or Crx+ cells residing near patches of Atoh7+ RPCs or Rbpms+ RGCs, respectively (Fig 6A–6N). Next, we quantified each nuclear marker and normalized using optic cup area (um^2, see Methods and S5 Table) for the different mutants. Surprisingly, the proportion of Atoh7 cells was largely normal, with significantly fewer cells in only Chx10-Cre; *Rbpj*$^{CKO/CKO}$ and Chx10-Cre;*Hes*^{TKO} eyes (Fig 6V). This did not correlate with the changes seen for either Rbpms+ RGCs or Crx+ photoreceptors (Fig 6Y). Although excess Pou4f+ RGCs were reported at E16 in a previous *Rbpj* conditional mutant study [14], here at E13.5 we found no difference in Rbpms+ RGCs, for either *Rbpj* mutant (Fig 6Y). It is plausible that ectopic RGCs in Rax-Cre;*Rbpj*$^{CKO/CKO}$ eyes might rapidly die (Fig 5P), and/or there is nonautonomous rescue in Chx10-Cre;*Rbpj*$^{CKO/CKO}$ eyes (S4E Fig). Alternatively, these RPCs may erroneously differentiate into neurons without fully committing to be an RGC, since there are obviously more Tubb3+ neurons in both *Rbpj* mutants, compared to control (Fig 6O–6U). Consistent with past studies of RGC genesis after blocking Notch signaling, we saw a significant increase in Rbpms+ cells for both sets of dnMAML and *Hes*^{TKO} mutants (Fig 6Y).

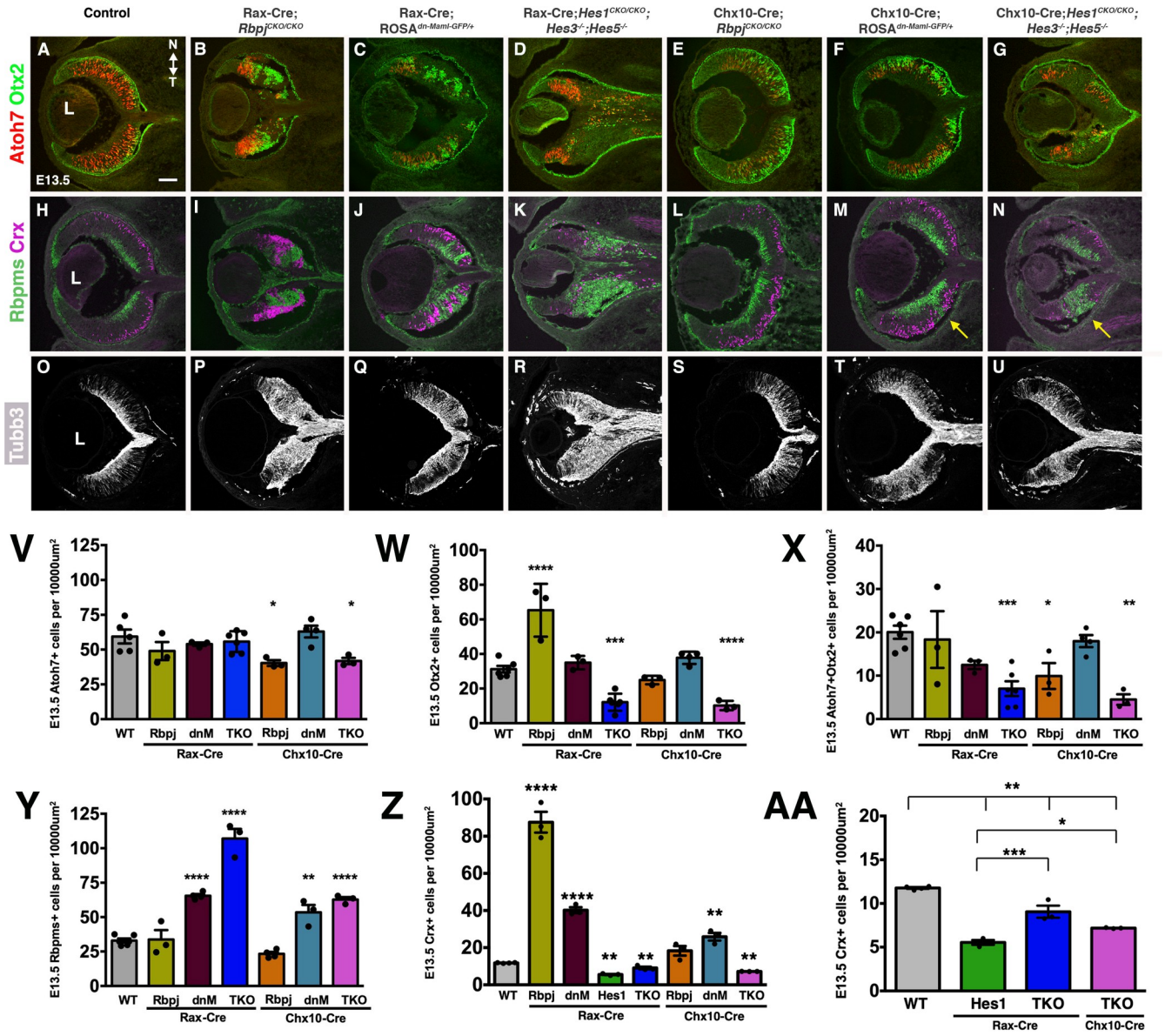

Fig 6. Shifts in RGC and early photoreceptor fates correlate with changes in Otx2, but not Atoh7, expression. (A-G) Atoh7-Otx2 double labeling at E13.5 highlights neurogenic defects across the allelic series and inappropriately labeled cells in D, where the retina had expanded. (H-N) E13.5 Rbpms-Crx double labeling reveals early mispatterning of RGCs (green) and photoreceptors (fuchsia). (O-U) Anti-Tubb3 labeling of E13 retinal sections emphasizes neurogenic phenotypes for all conditional mutants. All panels are oriented nasal up (noted in A), L = lens in A,H,O; scalebar in A = 50 microns. (V-Z) Quantification of Atoh7+ (V), Otx2+ (W), Atoh7+Otx2+ (X), Rbpms+ (Y), Crx+ (Z) nuclei normalized for optic cup area. Only Rax-Cre;*Rbpj* mutants have a significant increase in both Otx2+ and Crx+ cells; whereas both *Hes*^{TKO} mutants have a reduction of Otx2+ and Crx+ cells and an increase in Rbpms+ RGCs. (AA) Direct comparison of Crx+ cells for *Hes1* single versus *Hes*^{TKO} mutants (regraphed from panel Z) more clearly show a significant increase for both *Hes*^{TKO} mutants compared to the single mutant. Graph displays individual replicate data points normalized to optic cup area, the mean and S.E.M; Significant Welch's ANOVA, plus individual comparisons to wild type (*p< 0.05, **p<0.01, ***p<0.001, ****p <0.0001); n = 3 biologic replicates/genotype.

https://doi.org/10.1371/journal.pgen.1010928.g006

In contrast to Atoh7, the proportion of Otx2+ cells dramatically increased in Rax-Cre; *Rbpj*$^{CKO/CKO}$ mutants, and significantly decreased in *Hes*^{TKO} mutants, with no change for dnMAML (Fig 6W). Shifts in the subset of RPCs that typically express both competence factors also reflect that the impact is on Otx2 and not Atoh7 (compare Fig 6X to Fig 6V and 6W). By contrast, there was a big increase in Crx+ cells for Rax-Cre;*Rbpj*$^{CKO/CKO}$ mutants, with smaller, significant increases in most other genotypes (Fig 6Z). We also quantified Crx+ cells in Rax-

Cre;*Hes1*$^{CKO/CKO}$ mutants to facilitate direct comparison with both Cre-induced *Hes*^{TKO} mutants (Fig 6Z). This subset of data is regraphed in Fig 6AA to more easily see the partial rescue for both *Hes*^{TKO} mutants compared to single *Hes1* mutants. There was a simultaneous and significant increase in RGCs for all four *Hes*^{TKO} or dnMAML mutants (Fig 6Y). The largest increase in RGCs occurred in Rax-Cre;*Hes*^{TKO} eyes with expanded retinal tissue (Fig 3). Finally, it was surprising that the defects noted for Rbpms or Crx expressing cells correlate with significant changes in the cells expressing Otx2, but negatively correlate to the Atoh7+ population (Fig 6V–6X).

Direct comparison of both qualitative and quantitative defects in RGC versus Crx+ cohorts among the six mutants revealed other allele-specific defects during early retinogenesis. We found that only Rax-Cre;*Hes*^{TKO} mutants had displaced RGC and cone photoreceptor neurons in tissue that is normally optic stalk (Fig 6K). There were also mislocalized Rbpms+ RGCs in Chx-Cre;*ROSA*$^{dnMAML\text{-}GFP/+}$ and Chx10-Cre; *Hes*^{TKO} eyes, akin to interkinetic nuclear migration defects reported other Notch studies (arrow Fig 6M–6N) [74]. At E16.5, we noted that only Rax-Cre;*ROSA*$^{dnMAML\text{-}GFP/+}$ mutants contain more rosettes in the temporal retina (S6J Fig), suggesting a Notch-independent interaction occurred during N/T patterning that becomes more obvious over time.

It remains unclear why *Hes1* appears to promote cone genesis, rather than suppress it like other genes in the Notch pathway (Fig 6Z). One possibility is that *Hes1* regulates some aspect of cone versus rod fate choice, since postnatal *Hes1*$^{-/-}$ ex vivo retinal cultures were previously described to contain premature rod photoreceptor rosettes and fewer bipolar neurons [42]. First, we verified that at E16.5 the ectopic Crx+ cells in rosettes are Thrb2+ cones (S6A–S6N Fig) and not precocious Nr2e3+ rods [96–99]. Then we tested for premature rods within the Crx+ cohort. We collected E17 littermate control and Rax-Cre;*Hes1*$^{CKO/CKO}$ retinal sections and colabeled for Crx and Nr2e3, a transcription factor specifically found in nascent rods [96]. Nr2e3+ nuclei were evident within the forming outer nuclear layer (ONL) (S6O and S6P Fig) and retinal rosettes. However, the percentage of Nr2e3+Crx+ cells was identical (S6Q Fig). Therefore, the loss of cones in *Hes1* mutants cannot be attributed to accelerated rod genesis. Another explanation is that Hes1 provides temporal restriction to the Otx2 lineage to prevent prenatal bipolar neuron formation [100]. Alternatively, RGC development may accelerate in the absence of *Hes1*, depleting the availability of transitional RPCs to activate *Otx2* and adopt a cone fate.

Finally, we wished to understand why Rax-Cre;*Rbpj*$^{CKO/CKO}$ mutants overproduce Otx2+ and Crx+ cells in such vast excess (Fig 6W–6Z). A large subset of embryonic RPCs expresses the transcription factor *Otx2* and are initially capable of producing five fates: cone, rod, amacrine, horizontal or bipolar neurons [32–34]. However, Otx2 is shut off relatively quickly in those cells that will adopt amacrine and horizontal fates. The remaining Otx2-lineage cells, which produce cones, rods and bipolar neurons [22], then activate the transcription factor Crx [91,93,94,101]. When *Otx2* activity is blocked or removed, mutant cells switch from photoreceptor/bipolar to adopt amacrine/horizontal fates [32–34]. So, we evaluated another marker directly downstream of Otx2, Prdm1/Blimp1 [102,103], that is expressed before Crx. At, E13.5 Prdm1+ cells were quantified among all Rax-Cre induced mutants, plus Rax-Cre;*Hes1*$^{CKO/CKO}$ single and Rax-Cre;*Hes1*$^{CKO/CKO}$; *Hes3*$^{+/-}$;*Hes5*$^{+/-}$ mutants for better evaluation of the relative contributions of each *Hes* gene (Fig 7A–7F and 7M). We found the greatest excess of Prdm1+ cells in *Rbpj* mutants, compared with a modest increase in Rax-Cre; *ROSA*$^{dnMAML\text{-}GFP/+}$ eyes and a significant reduction in *Hes1* single or triple mutants (Fig 7M). This outcome for Prdm1 further confirms the Otx2 and Crx data, suggesting that *Rbpj* and *Hes1* act differently upstream of Otx2.

Within the early Otx2 lineage, cells transiting to amacrine or horizontal fates downregulate Otx2 as they activate the transcription factor Ptf1a [reviewed in 104]. Ptf1a is both necessary

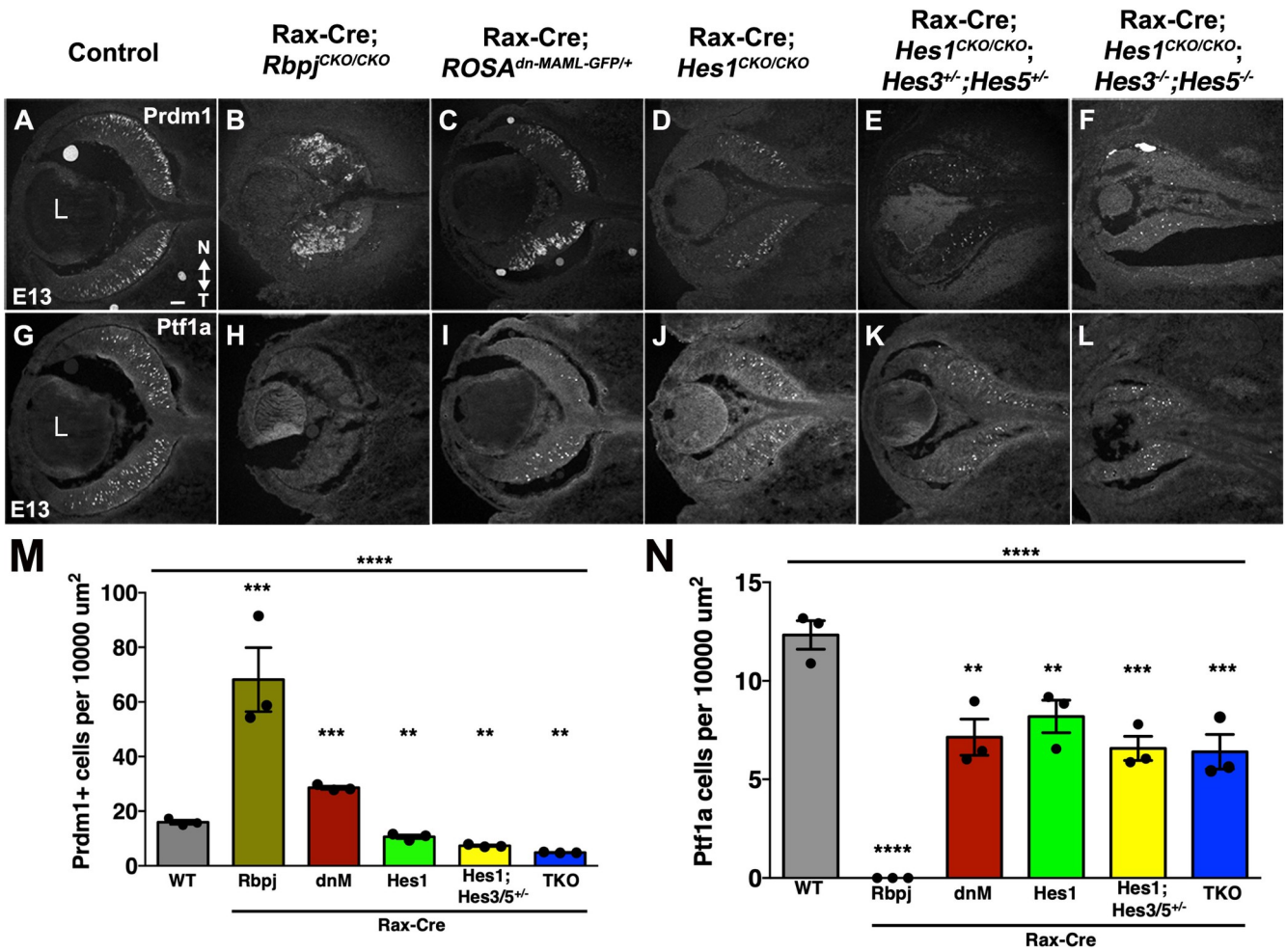

Fig 7. Unique role for *Rbpj* in regulation photoreceptor versus amacrine fates. Prdm1/Blimp1 (A-F) and Ptf1a (G-L) labeling of E13.5 Rax-Cre-meditated deletion of Notch pathway genes. (M,N) Strikingly, *Rbpj* mutants have both excess Prdm1+ cells and a total loss of Ptf1a-expressing cells. All other genotypes exhibit significant, but smaller, shifts in labeled populations. Graphs display individual replicate data points, the mean and S.E.M; Significant Welch's ANOVA (****p< 0.0001; and pairwise comparisons to wild type (***p<0.001, ** p< 0.01). All panels oriented nasal up (noted in A), with L = lens in A,G; scalebar in A = 50 microns; n = ≥3 biological replicates/genotype.

https://doi.org/10.1371/journal.pgen.1010928.g007

and sufficient for amacrine and horizontal fates, and when retinal cells lose this factor, they erroneously develop as RGCs and photoreceptors [105–107]. Without *Rbpj* there was a total loss of Ptf1a+ cells (Fig 7H–7N). By contrast the other mutants had only a partial loss of Ptf1a + cells, likely reflecting a generally reduced pool of RPCs (Fig 7N). The more severe consequences of removing *Rbpj* on the amacrine pathway agree with previous studies (S1 Table), and further reinforce that Ptf1a expression depends on *Rbpj*, similar to Ptf1a target genes [17,105,107].

Discussion

The molecular mechanisms integrating Notch with other signaling pathways remain poorly understood. Here we directly compared the genetic requirements for ternary complex components and multiple *Hes* genes during ONH formation and the onset of retinal neurogenesis (Fig 8A). We found that only *Hes1* is required in the ONH. While all genes examined control RPC proliferation, our findings also point to particular Notch-independent activities.

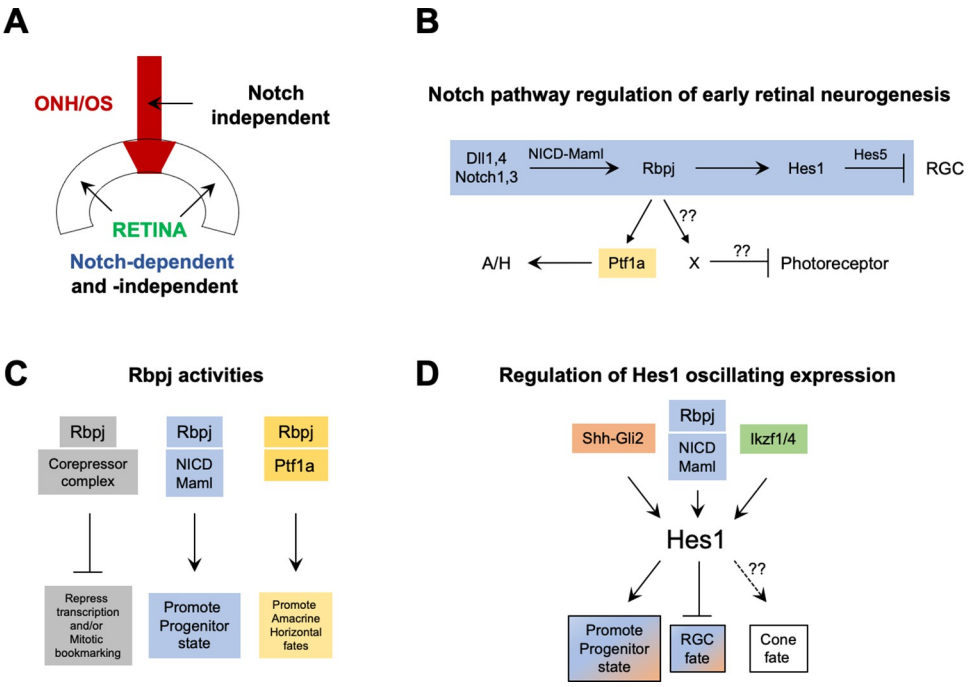

Fig 8. Notch pathway activities and integration points with other genetic pathways in the embryonic eye. (A) Sustained Hes1 expression in the ONH/OS does not require ternary complex gene activities (Notch-independent). RPC status and early retinal fates are Notch-dependent, but also require other inputs. (B) Canonical Notch signal (blue) blocks premature RGC differentiation, while noncanonical Rbpj activity (yellow) utilizes Notch-independent modes to also regulate photoreceptor versus amacrine/horizontal fate (A/H). (C) The Rbpj protein forms distinct protein complexes (three shown) that uniquely regulate transcription and cell fates. By sequestering Rbpj into the different complexes, the production of one cell type also impacts its availability to regulate the other early cell types. (D) Distinct Hes1 transcriptional regulators influence oscillating Hes1 expression and activity during retinal neurogenesis. Since Hes1 encodes a repressor protein, its positive effect on cones is predicted to be indirect, presumably blocking and unknown factor X that normally suppresses cone genesis.

https://doi.org/10.1371/journal.pgen.1010928.g008

Although *Hes1* and *Hes5* transcriptional repressors have been compared using a variety of tools, their potential redundancy in the eye had not been tested [11,14,18,42,50,51,59,60]. *Hes1* maintains optic vesicle and cup growth, the tempo of retinogenesis, and promotes astrocyte development in ONH/OS cells. But paralogues *Hes3* and *Hes*5 have only subtle roles [18,108]. In other areas of the CNS, *Hes3* is active during oligodendrocyte maturation and interacts with STAT3-Ser and Wnt signaling pathways prior to the initiation of myelination [109,110]. Given that *Hes3* mRNA is undetectable in the embryonic retina, we propose it is relatively more important postnatally, possibly for retinal astrocyte migration, or optic nerve myelination.

Making and keeping the retinal-glial boundary

The boundary between the retina and OS possesses many characteristics of the brain isthmus, which is comprised of slowly proliferating cells that undergo little to no neurogenesis and act as a signaling hub for adjacent neural tissues [reviewed in 39,111]. Consistent with this idea, we found *Hes1* is required for Ccnd2 expression, which is associated with prolonged cell cycles. Both the ONH and isthmus require the transcription factors *Hes1* and *Pax2*. In the eye, loss of either gene allows the retina to encroach and displace the ONH. This expansion might be due to a failure to effectively shift from fast to slow cycling kinetics or be driven by ectopic *Hes5* plus other early eye factors. In this specific context, Rax-Cre;Hes^{TKO} eyes were not much different than the loss of *Hes1* alone. Thus, sustained *Hes1* is likely sufficient for ONH formation

and maintenance. We found no role for Notch regulation in ONH/OS formation since both *Rbpj* and *ROSA*$^{dnMAML\text{-}GFP/+}$ animals retain a recognizable ONH with sustained Hes1 expression (Fig 8A).

Hes1 expression in the ONH/OS must be regulated by other genetic pathways. A strong candidate is the Shh pathway. Shh signaling performs an important feedback mechanism to control RGC population size. Nascent RGCs secrete Shh, which instructs RPCs to remain mitotically active via direct binding of Gli2 to activate *Hes1* transcription [52,112]. Moreover, at the optic vesicle stage of development, Shh diffuses from the ventral diencephalon midline to stimulate outgrowth of the optic cup and stalk [reviewed in 113]. Given that Wnt, Bmp and Retinoic Acid signals also regulate proximoventral optic cup and stalk outgrowth and specification [reviewed in 114], it is tantalizing to speculate that they do so by converging on Hes1 expression and/or activity. It also remains unresolved if the ONH is a signaling hub for the adjacent retina.

To delineate ONH versus retinal phenotypes, we used both Rax-Cre and Chx10-Cre drivers to test for functional redundancy of *Hes1* and *Hes5* during retinal neurogenesis. Unfortunately, the Chx10-Cre line could only produce a few robust outcomes. This was unanticipated since the Chx10-Cre driver was successfully used in past retinal analyses of *Dll1*, *Notch1*, *Hes1*, *Rbpj* and *Neurog2* function [10,13–16,50,115]. Due to mosaic expression and because fewer and fewer Cre-GFP+ cells are present as development progresses, we expect that selection pressure favored wild-type cells and their nonautonomous rescue of some of the phenotypes. Nonetheless, we uncovered distinct *Hes*^{TKO} phenotypes using these Cre drivers at E13.5. Only Rax-Cre;*Hes*^{TKO} mutants had a specific displacement of retinal tissue into the OS. The Pax6/Pax2 double positive cohort, along the retina-ONH boundary was largely missing, but the size of the mispositioned ONH was relatively normal (Fig 3). By contrast, Chx10-Cre;*Hes*^{TKO} mutants had a bigger Pax2 domain, further confirmed by expansion of the Vax1 ONH marker into neural retinal territory. Our interpretation is that the earlier, broader Rax-Cre mutant prevented ONH/OS cells from adopting distinct identities, thus cells remained OC-like longer, producing more retinal tissue. This is likely a Hes1-specific process. But in Chx10-Cre mutants, with Cre expression restricted to the neural side of the boundary and acting at a slightly older age, the redundant, neurogenic role of *Hes5* was revealed, since the retinal cells coexpressed neuronal and optic-stalk markers. Interestingly both phenotypes are apparent in *Pax2* mutants, suggesting that *Pax2* is upstream of Hes5, but acts parallel to *Hes1*. Future multiomic studies that characterize ONH cells, in the absence of *Hes1* or *Pax2*, will be very informative. Finally our data highlight the variable penetrance and severity of Rax-Cre versus Chx10-Cre drivers, which is instructive for future studies.

Multiple modes regulating retinal histogenesis

Another important goal of this study was to understand how precisely *Hes1* and *Hes5* activities mirror the Notch ternary complex, which directly activates *Hes* gene transcription [reviewed in 4]. Because there are multiple ligands and Notch receptors expressed in the developing retina (Fig 8B), we focused on the requirements for *Rbpj* (Fig 8C) and to a lesser extent *Maml*. There are three *Mastermind-like* paralogues (*Maml* genes), but germline mutant analyses failed to uncover individual gene functions during embryogenesis [reviewed in 116]. Subsequently, a dominant negative isoform of MAML1 (dnMAML) was created, in which the MAML1 N-terminus forms ternary complexes with NICD and Rbpj, but cannot further interact with obligate transcriptional coactivators (e.g., p300, histone acetyltransferases) [54–57]. This has been a powerful tool in cancer biology and immunology research [54], but during retinal neurogenesis, dnMAML is less effective at blocking Notch signaling. This might be attributed to

differences in expression levels relative to other studies (in vivo Cre-mediated induction here, versus plasmid or viral delivery). However, several dnMAML eye defects, namely temporal retina-specific downregulation of Hes1 and *Hes5*, Foxg1 mislocalization and an unequal appearance of photoreceptor rosettes (Figs 2, S5 and S6J) suggest that Rax-Cre;$ROSA^{dnMAML\text{-}GFP/+}$ mutants have Notch-independent genetic interactions. In vitro proteomic studies support this idea, where dnMAML can bind to Gli and Tcf/Lef proteins [117,118]. This implies that $ROSA^{dnMAML\text{-}GFP/+}$ retinal phenotypes may represent composite outcomes of simultaneously interfering with Notch, Shh, and/or Wnt signaling.

Rbpj also has Notch-independent functions (Fig 8C), the most common being its role in co-repressor protein complexes to silence transcription via DNA methylation [reviewed in 4]. Another activity is through Rbpj interactions with Ptf1a-E47 in a higher order PTF1 complex that has been studied in the pancreas, spinal cord and retina [104]. In the pancreas, PTF1 complexes can activate *Dll1*, suggesting as a feedback loop from postmitotic to mitotic cells, via Dll1 binding to Notch1 [119]. PTF1 can also directly antagonize Notch signaling in a cell autonomous and dose-dependent manner, since Ptf1a and NICD bind to the same site on the Rbpj protein [104,120]. The second scenario is likely more relevant here. It is plausible that in the retina, when a critical threshold of Rbpj protein is bound up in PTF1 complexes, it not only impacts Rbpj availability for active Notch ternary complexes, but diverts cells from photoreceptor fate choice. We conclude that *Rbpj* activity regulates early photoreceptor development in at least two ways. First, in the Notch-dependent ternary complex, *Rbpj* controls RPC division versus differentiation into neurons like photoreceptors. Second, independent of Notch, *Rbpj* prevents cells normally destined to become amacrines from erroneously developing as photoreceptors via regulation of and independent physical interaction with Ptf1a (Fig 8B and 8C).

These additional *Rbpj* and *Hes1* functions significantly complicate meaningful interpretation of our genetic data concerning Notch signaling regulation of *Otx2*. For *Rbpj* mutants, the expansion of Otx2+, Crx+, Prdm1+ cells, and cones, at the expense of Ptf1a and amacrine neurons, fits current models of mutual exclusion mentioned above [reviewed in 104]. Conversely, *Hes1* mutants produce excess RGCs and too few cones, which is essentially the opposite of *Rbpj* mutants. This might be attributed to *Hes1* loss being relatively more efficient than *Rbpj*, facilitating RPC adoption of RGC fate, which also depletes the pool available for photoreceptor formation. Alternatively, Hes1 and Rbpj may simultaneously regulate (via distinct Notch-independent activities), competence or differentiation factors, for example *Atoh7* [14,50,121]. Here we found that Atoh7 protein expression is not correlative with RGC differentiation, in agreement with, single cell transcriptomics data [24]. Instead, other competence factors, like Otx2, fluctuate as transitional RPCs adopt RGC or cone fates, with Otx2 expression becoming permanent in nascent and differentiated photoreceptors [33,34]. Does this mean that the absence of Otx2 is needed for RGC fate? We propose that the Notch genes tested here, via different modes of action, act upstream of Otx2, to influence cell cycle status while also potentially targeting other genes that enable or limit RGC formation.

When considered together, our data and other studies, point to *Hes1* as a signal integration point (Fig 8D). *Hes1* mRNA and protein are dynamic, and likely important for the establishment of cellular heterogeneity. Hes1 might convey pulsatile feedback to other oscillating molecules like *Dll1*, *Neurog2* or *Ascl1* [40,41], which could occur upstream of *Otx2*. Although circumstantial, Prdm1+ cells and rods are specifically reduced in postnatal *Neurog2* mutants, but how directly these events are linked remains to be determined [88,115]. Future studies that apply short-lived Hes reporters and single cell imaging and sequencing modalities to remaining questions about when and where Notch signaling is required will be illuminating.

Materials and methods

Ethics statement

All mice were housed and cared for in accordance with guidelines provided by the National Institutes of Health and the Association for Research in Vision and Ophthalmology, and conducted with approval and oversight from the UC Davis Institutional Animal Care and Use Committee (Protocols #20065 and #21839).

Animals

Mouse strains used in this study are Hes5-GFP BAC transgenic line (*Tg(Hes5-EGFP) CV50Gsat/Mmmh* line; stock 000316-MU) [60,122]; *Hes1*^{CKO} allele (*Hes1*^{tm1Kag}) maintained on a CD-1 background [53]; *Rbpj* $^{CKO/CKO}$ (*Rbpj*^{tm1Hon}) on a *C57BL/6J* background[8]; *Pax2*$^{GFP/+}$ (*Pax2*$^{tm1.1Gdr}$) maintained on a CD-1 background [123]; ROSA26$^{dnMAML\text{-}GFP}$ (*Gt(ROSA)26Sor*$^{tm1(MAML1)Wsp}$) maintained on a C57BL/6J background [54–57]; *Hes1*$^{CKO/CKO}$; *Hes3*$^{-/-}$;*Hes5*$^{-/-}$ (*Hes1*^{tm1Ka})(*Hes3*^{tm1Kag}) (*Hes5*^{tm1Fgu}) triple homozygous stock, maintained on CD-1 and termed "*TKO*" in this study [43,53]; *Hes3*$^{-/-}$;*Hes5*$^{-/-}$ mice, derived from the triple stock, with loss of *Hes3* and *Hes5* mRNA validated by whole mount in situ hybridization at E10.5; Chx10-Cre BAC transgenic line (*Tg Chx10-EGFP/cre;-ALPP)2Clc*; JAX stock number 005105) maintained on a CD-1 background [58]; and Rax-Cre BAC transgenic line (Tg(Rax-cre) NL44Gsat/Mmucd created by the GENSAT project [122], cryobanked at MMRRC UC Davis (Stock Number: 034748-UCD), and maintained on a CD-1 background. PCR genotyping was performed as described [8,43,53–58,60,122,123]. Conditional mutant breeding schemes mated one heterozygous Cre mouse to another mouse homozygous for the GeneX conditional allele to create Cre;*GeneX*$^{CKO/+}$ mice. The Cre;*GeneX*$^{CKO/+}$ mice were used in timed matings with *GeneX*$^{CKO/CKO}$ mice (see S2 Table) and littermates lacking Cre were used as controls throughout this study. The date of a vaginal plug was assigned the age of E0.5.

Histology and immunofluorescent labeling

P21 eyes were dissected and fixed in 4% paraformaldehyde/PBS overnight at 4˚C then processed through standard dehydration steps and paraffin embedding. Four micron sections were deparaffinized using Histoclear II (National Diagnostics HS200), hydrated through graded ethanol series and either stained with Hematoxylin and Eosin (H&E), or underwent antigen unmasking in hot (95˚C) 0.01M sodium citrate for 20 minutes, prior to immunofluorescent staining and imaging. For cryosection immunofluorescence, embryonic heads were fixed in 4% paraformaldehyde/PBS for 1 hour on ice, processed by stepwise sucrose/PBS incubations, and embedded in Tissue-Tek OCT. Ten micron frozen sections were labeled as in [78] with primary and secondary antibodies listed in S3 and S4 Tables. Nuclei were counterstained with DAPI.

RNA *in situ* hybridization

DIG-labeled antisense riboprobes were synthesized from mouse *Hes5* [60], and mouse *Vax1* [85] cDNA templates. In situ probe labeling, cryosection hybridizations and color development were performed using published protocols [26,124].

Microscopy and statistical analysis

Histologic and in situ hybridization sections were imaged with a Zeiss Axio Imager M.2 microscope, color camera and Zen software (v2.6). Antibody-labeled cryosections were imaged using a Leica DM5500 microscope, equipped with a SPEII solid state laser scanning confocal

and processed using Leica LASX (v.5) plus Navigator tiling subprogram, FIJI/Image J Software (NIH) and Adobe Photoshop (CS5) software programs. All images were equivalently adjusted for brightness, contrast, and pseudo-coloring. At least 3 biologic replicates per age and genotype were analyzed for every marker, and 1–2 sections per individual were quantified via cell counting and retinal tissue area measurements (S5 Table). Sections were judged to be of equivalent depth by presence of or proximity to the optic nerve and/or characteristics of the adjacent forming lens. To normalize marker quantifications relative to tissue morphology changes, we calculated the square area (um^2) of retinas from E13 sections, using FIJI (NIH) to trace a polygon, excluding the opening for the optic nerve [125]. The average number of marker+ cells were divided by the square micron area of the retina and graphed using Prism (GraphPadv9). For E17 retina, 11 tile scanned retinal sections for each of 3 biologic replicates/genotype were quantified, using the count tool in Adobe Photoshop CS5. Statistical analyses were performed on cells counts (S5 Table) using Prism (GraphPad v9) or Excel (v16.16.11) software, with p-values determined using one-way ANOVA and pair-wise Dunnett or pair-wise Whitney test or a Student's T-test. p-values less than 0.05 were considered statistically significant.

Supporting information

S1 Table. Summary of Notch pathway mutant phenotypes in mouse retina.
(DOCX)

S2 Table. Recovery of mutant embryos/neonates at relevant stages of eye development.
(DOCX)

S3 Table. Validated primary antibody markers.
(DOCX)

S4 Table. Secondary antibody reagents.
(DOCX)

S5 Table. Numerical datasets underlying all graphs.
(XLSX)

S1 Fig. *Hes3*$^{-/-}$;*Hes5*$^{-/-}$ double mutants have no discernible eye phenotypes. (A,B) Number and pattern of Pou4f+ RGCs is unaltered at E13.5. (C,D) Pax6+ RPCs and mitotic Ccnd1+ cells are unaffected at E13.5. (E,F) Cdkn1b+ postmitotic RGCs and Sox9+ RPCs, RPE and ONH cells are the same between control and double mutants at E13.5. (G-J) Adult (P28) Müller glia, labeled with Sox9 (G,H) or Rlpb1/CRALBP (I,J) are also normal. All panels are vitreal down, scleral up; scalebar in A, E = 20 microns; n = 4 biologic replicates/genotype.
(TIF)

S2 Fig. *Hes5* mRNA expression in E16.5 *Hes1* conditional mutants. A-C) *Hes5* inappropriately expands into the optic stalk (OS) when *Hes1* is conditionally removed with Rax-Cre (arrow in C), but not Chx10-Cre (B). L = lens; CM = ciliary margin; RPC = retinal progenitor cells; ONH = optic nerve head. Bar = 100 microns; n $\geq$3 per genotype.
(TIF)

S3 Fig. P21 Hes triple mutants are more severe than *Hes1* single mutants. (A-D) H&E staining highlights a range of ocular defects in adult eyes. Boxed areas at higher magnification in inset. (B) Without *Hes1* an ectopic vitreal cell mass resides next to the ONH and there are sporadic retinal rosettes. (C-D) Chx10-Cre;*Hes*^{TKO} eyes have more extensive retinal lamination defects and abnormal ONH morphology. (E-L') Colabeling for Tubb3 (green, neuronal

processes) and Endomucin (red, endothelial cells). (I-L') Higher magnification of boxed areas in E-H. Endomucin labeling of choroid vessels (white arrows) and blood vessels within abnormal vitreal cell masses (pink arrows). This ectopic tissue is largely devoid of Tubb3+ neurons or neural processes. Panels E,I,I' are of an adjacent section to A; panels G,K,K' are an adjacent section to C; panels H,L,L' are an adjacent section to D. Asterisks in I, I' or J,J' indicate autofluorescent photoreceptor outer segments or red blood cells within ectopic vessels. Scalebars in A = 200 microns, E,I = 20 microns; n = 3 biologic replicates per genotype.
(TIF)

S4 Fig. Relative efficiencies of Rax-Cre versus Chx10-Cre BAC Tg drivers. (A-A') Normal E13.5 expression patterns for Rbpj and Hes1. (B-B") Complete loss of *Rbpj* in Rax-Cre lineage-marked cells (optic cup, RPE, ONH, OS) in red, see B'. There was also a loss of Hes1 in the cup and RPE, but not in the attenuated ONH/OS (B"). (C-D') Anti-Rbpj and GFP labeling highlights Chx10-Cre-GFP mosaicism, with scattered GFP-negative retinal cells (red only nuclei in C, pink only in D). Chx10-Cre expression does not spread into the ONH (D). (E-F') In Chx10-Cre;*Rbpj* mutant littermates, Rbpj+ cells are dramatically reduced, although the Hes1 retinal domain is less effected (F). Hes1 in the ONH is unaffected in Chx10-Cre animals as expected. (G-H') At E16, Cre-GFP, Rbpj and Hes1 are normally coexpressed. (I-J') Proportionally bigger Cre-GFP-neg regions of Chx10-Cre;*Rbpj* mutant retinas express Rbpj. In J, islands of GFP+ mutant cells are surrounded by Hes1-expressing cells, which either did not undergo Cre recombination or are wild type cells that eventually outcompete and subsequently outnumber the mutant cells. Scalebar in A, C = 50 microns, L = lens in A,B; n = 3 biologic replicates/genotype.
(TIF)

S5 Fig. Nasal-temporal patterning is normal in *Notch* pathway mutants. (A-G) At E13.5 Foxg1, in the nasal retina, is properly patterned among nearly all mutants. Only Rax-Cre; Hes^{TKO} eyes (D), showed Foxg1 expansion into the optic stalk, consistent with other RPC markers (Figs 1G,3D,3K), where it remained biased to the nasal portion of the retina and optic stalk. (H-M) At E16.5, all mutants have nasally-restricted Foxg1 expression, except Rax-Cre; $ROSA^{dnMAML1\text{-}GFP/+}$ retinas that have some Foxg1+ nuclei present on the temporal side and within the adjacent subretinal space (arrow in J). All panels oriented nasal up (noted in A) and brain to the right; with L = lens in A,H; scalebar in A, H = 50 microns; n = 3 biologic replicates/genotype.
(TIF)

S6 Fig. E16.5 Notch pathway mutant cone photoreceptor rosettes. (A-G) Immunostaining for the cone-specific Thrb2 marker at E16.5. (H-N) Crx-Rbpms colabeling of adjacent E16.5 sections highlights the abundance of RGCs and cones relative to other unlabeled cells, as well as photoreceptor rosettes surrounded by RGCs. Panels A-N oriented nasal up, n = $\geq$3 biological replicates/genotype. (O,P) Crx-Nr2e3 double labeling of E17.5 control and Rax-Cre; $Hes1^{CKO/CKO}$ retinas. (Q) Quantification of colabeled cells within the Crx population indicates no difference in nascent Nr2e3+ rods between genotypes. Panels A-N oriented nasal up (indicated in A), panels O,P oriented scleral up; graphical data in Q represents 13 control and 11 tile scanned composite images from 3 biologic replicates/genotype, displaying individual replicate data points, mean and standard deviation. A student t-test, with unequal variance was used to calculate a p-value in Q. Scalebars in A = 50 microns, P = 20 microns, L = lens in A,H; ONL = outer nuclear layer.
(TIF)

Acknowledgments

The authors thank Ryoichiro Kageyama, Tasuko Honjo, and Ivan Maillard for mutant mouse strains; Doug Forrest for Thrb2 antibody; Cheryl Craft for Opsin antibodies; Chris Wright for Ptf1a antibody; Brad Shibata and Paul FitzGerald for assistance with histology; Amy Riesenberg, April Bird, Kelly McCulloh for technical support. The authors also thank Anna La Torre and Tom Glaser for thoughtful comments and members of the UCD Friday Eye Development group for critical feedback and discussion.

Author Contributions

Conceptualization: Joseph A. Brzezinski IV, Nadean L. Brown.

Data curation: Nadean L. Brown.

Formal analysis: Bernadett Bosze, Julissa Suarez-Navarro, Illiana Cajias, Joseph A. Brzezinski IV, Nadean L. Brown.

Funding acquisition: Nadean L. Brown.

Investigation: Bernadett Bosze, Julissa Suarez-Navarro, Illiana Cajias, Joseph A. Brzezinski IV, Nadean L. Brown.

Methodology: Bernadett Bosze, Julissa Suarez-Navarro, Illiana Cajias, Joseph A. Brzezinski IV, Nadean L. Brown.

Project administration: Nadean L. Brown.

Resources: Nadean L. Brown.

Supervision: Nadean L. Brown.

Validation: Nadean L. Brown.

Writing – original draft: Bernadett Bosze, Nadean L. Brown.

Writing – review & editing: Bernadett Bosze, Julissa Suarez-Navarro, Joseph A. Brzezinski IV, Nadean L. Brown.

References

1. Hufnagel RB, Brown NL. Specification of Retinal Cell Types. In: Rubenstein JLR P. R, editors. Comprehensive Developmental Neuroscience: Patterning and Cell Type Specification in the Developing CNS and PNS. 1. Amsterdam: Elsevier; 2013. p. 519–36.
2. Shiau F, Ruzycki PA, Clark BS. A single-cell guide to retinal development: Cell fate decisions of multipotent retinal progenitors in scRNA-seq. Dev Biol. 2021; 478:41–58. Epub 2021/06/20. https://doi.org/10.1016/j.ydbio.2021.06.005 PMID: 34146533; PubMed Central PMCID: PMC8386138.
3. Greenwald I, Kovall R. Notch signaling: genetics and structure. WormBook. 2013:1–28. Epub 2013/01/29. https://doi.org/10.1895/wormbook.1.10.2 PMID: 23355521.
4. Kovall RA, Gebelein B, Sprinzak D, Kopan R. The Canonical Notch Signaling Pathway: Structural and Biochemical Insights into Shape, Sugar, and Force. Developmental cell. 2017; 41(3):228–41. Epub 2017/05/10. https://doi.org/10.1016/j.devcel.2017.04.001 PMID: 28486129; PubMed Central PMCID: PMC5492985.
5. Nam Y, Weng AP, Aster JC, Blacklow SC. Structural requirements for assembly of the CSL.intracellular Notch1.Mastermind-like 1 transcriptional activation complex. J Biol Chem. 2003; 278(23):21232–9. Epub 2003/03/20. https://doi.org/10.1074/jbc.M301567200 PMID: 12644465.
6. Wilson JJ, Kovall RA. Crystal structure of the CSL-Notch-Mastermind ternary complex bound to DNA. Cell. 2006; 124(5):985–96. Epub 2006/03/15. https://doi.org/10.1016/j.cell.2006.01.035 PMID: 16530045.

7. Hu N, Zou L. Multiple functions of Hes genes in the proliferation and differentiation of neural stem cells. Annals of Anatomy—Anatomischer Anzeiger. 2022; 239:151848. https://doi.org/10.1016/j.aanat.2021.151848 PMID: 34715307

8. Han H, Tanigaki K, Yamamoto N, Kuroda K, Yoshimoto M, Nakahata T, et al. Inducible gene knockout of transcription factor recombination signal binding protein-J reveals its essential role in T versus B lineage decision. Int Immunol. 2002; 14(6):637–45. https://doi.org/10.1093/intimm/dxf030 PMID: 12039915.

9. Jadhav AP, Cho SH, Cepko CL. Notch activity permits retinal cells to progress through multiple progenitor states and acquire a stem cell property. Proc Natl Acad Sci U S A. 2006; 103(50):18998–9003. Epub 2006/12/07. https://doi.org/10.1073/pnas.0608155103 PMID: 17148603; PubMed Central PMCID: PMC1682012.

10. Jadhav AP, Mason HA, Cepko CL. Notch 1 inhibits photoreceptor production in the developing mammalian retina. Development. 2006; 133(5):913–23. https://doi.org/10.1242/dev.02245 PMID: 16452096.

11. Maurer KA, Riesenberg AN, Brown NL. Notch signaling differentially regulates Atoh7 and Neurog2 in the distal mouse retina. Development. 2014; 141(16):3243–54. Epub 2014/08/08. https://doi.org/10.1242/dev.106245 PMID: 25100656; PubMed Central PMCID: PMC4197552.

12. Mizeracka K, DeMaso CR, Cepko CL. Notch1 is required in newly postmitotic cells to inhibit the rod photoreceptor fate. Development. 2013; 140(15):3188–97. Epub 2013/07/05. https://doi.org/10.1242/dev.090696 PMID: 23824579; PubMed Central PMCID: PMC3931735.

13. Riesenberg AN, Brown NL. Cell autonomous and nonautonomous requirements for Delltalike1 during early mouse retinal neurogenesis. Dev Dyn. 2016; 245(6):631–40. Epub 2016/03/08. https://doi.org/10.1002/dvdy.24402 PMID: 26947267; PubMed Central PMCID: PMC4873400.

14. Riesenberg AN, Liu Z, Kopan R, Brown NL. Rbpj cell autonomous regulation of retinal ganglion cell and cone photoreceptor fates in the mouse retina. J Neurosci. 2009; 29(41):12865–77. https://doi.org/10.1523/JNEUROSCI.3382-09.2009 PMID: 19828801; PubMed Central PMCID: PMC2788434.

15. Rocha SF, Lopes SS, Gossler A, Henrique D. Dll1 and Dll4 function sequentially in the retina and pV2 domain of the spinal cord to regulate neurogenesis and create cell diversity. Dev Biol. 2009; 328(1):54–65. https://doi.org/10.1016/j.ydbio.2009.01.011 PMID: 19389377.

16. Yaron O, Farhy C, Marquardt T, Applebury M, Ashery-Padan R. Notch1 functions to suppress cone-photoreceptor fate specification in the developing mouse retina. Development. 2006; 133(7):1367–78. https://doi.org/10.1242/dev.02311 PMID: 16510501.

17. Zheng MH, Shi M, Pei Z, Gao F, Han H, Ding YQ. The transcription factor RBP-J is essential for retinal cell differentiation and lamination. Molecular brain. 2009; 2:38. https://doi.org/10.1186/1756-6606-2-38 PMID: 20017954; PubMed Central PMCID: PMC2804697.

18. Furukawa T, Mukherjee S, Bao ZZ, Morrow EM, Cepko CL. rax, Hes1, and notch1 promote the formation of Muller glia by postnatal retinal progenitor cells. Neuron. 2000; 26(2):383–94. Epub 2000/06/06. https://doi.org/10.1016/s0896-6273(00)81171-x PMID: 10839357.

19. Henrique D, Hirsinger E, Adam J, Le Roux I, Pourquie O, Ish-Horowicz D, et al. Maintenance of neuroepithelial progenitor cells by Delta-Notch signalling in the embryonic chick retina. Curr Biol. 1997; 7(9):661–70. https://doi.org/10.1016/s0960-9822(06)00293-4 PMID: 9285721.

20. Bao ZZ, Cepko CL. The expression and function of Notch pathway genes in the developing rat eye. J Neurosci. 1997; 17(4):1425–34. https://doi.org/10.1523/JNEUROSCI.17-04-01425.1997 PMID: 9006984.

21. Scheer N, Groth A, Hans S, Campos-Ortega JA. An instructive function for Notch in promoting gliogenesis in the zebrafish retina. Development. 2001; 128(7):1099–107. Epub 2001/03/14. https://doi.org/10.1242/dev.128.7.1099 PMID: 11245575.

22. Brzezinski JA, Reh TA. Photoreceptor cell fate specification in vertebrates. Development. 2015; 142(19):3263–73. https://doi.org/10.1242/dev.127043 PMID: 26443631

23. Ge Y, Chen X, Nan N, Bard J, Wu F, Yergeau D, et al. Key transcription factors influence the epigenetic landscape to regulate retinal cell differentiation. Nucleic acids research. 2023; 51(5):2151–76. Epub 2023/01/31. https://doi.org/10.1093/nar/gkad026 PMID: 36715342; PubMed Central PMCID: PMC10018358.

24. Wu F, Bard JE, Kann J, Yergeau D, Sapkota D, Ge Y, et al. Single cell transcriptomics reveals lineage trajectory of retinal ganglion cells in wild-type and Atoh7-null retinas. Nat Commun. 2021; 12(1):1465. Epub 2021/03/07. https://doi.org/10.1038/s41467-021-21704-4 PMID: 33674582; PubMed Central PMCID: PMC7935890.

25. Clark BS, Stein-O'Brien GL, Shiau F, Cannon GH, Davis-Marcisak E, Sherman T, et al. Single-Cell RNA-Seq Analysis of Retinal Development Identifies NFI Factors as Regulating Mitotic Exit and Late-

Born Cell Specification. Neuron. 2019; 102(6):1111–26 e5. Epub 2019/05/28. https://doi.org/10.1016/j.neuron.2019.04.010 PMID: 31128945.

26. Brown NL, Kanekar S, Vetter ML, Tucker PK, Gemza DL, Glaser T. Math5 encodes a murine basic helix-loop-helix transcription factor expressed during early stages of retinal neurogenesis. Development. 1998; 125(23):4821–33. https://doi.org/10.1242/dev.125.23.4821 PMID: 9806930.

27. Miesfeld JB, Glaser T, Brown NL. The dynamics of native Atoh7 protein expression during mouse retinal histogenesis, revealed with a new antibody. Gene Expr Patterns. 2018; 27:114–21. Epub 2017/12/12. https://doi.org/10.1016/j.gep.2017.11.006 PMID: 29225067; PubMed Central PMCID: PMC5835195.

28. Brown NL, Patel S, Brzezinski J, Glaser T. Math5 is required for retinal ganglion cell and optic nerve formation. Development. 2001; 128(13):2497–508. https://doi.org/10.1242/dev.128.13.2497 PMID: 11493566; PubMed Central PMCID: PMC1480839.

29. Brzezinski JAt, Prasov L, Glaser T. Math5 defines the ganglion cell competence state in a subpopulation of retinal progenitor cells exiting the cell cycle. Dev Biol. 2012; 365(2):395–413. https://doi.org/10.1016/j.ydbio.2012.03.006 PMID: 22445509; PubMed Central PMCID: PMC3337348.

30. Wang SW, Kim BS, Ding K, Wang H, Sun D, Johnson RL, et al. Requirement for math5 in the development of retinal ganglion cells. Genes Dev. 2001; 15(1):24–9. Epub 2001/01/13. https://doi.org/10.1101/gad.855301 PMID: 11156601; PubMed Central PMCID: PMC312600.

31. Kanekar S, Perron M, Dorsky R, Harris WA, Jan LY, Jan YN, et al. Xath5 participates in a network of bHLH genes in the developing Xenopus retina. Neuron. 1997; 19(5):981–94. Epub 1997/12/09. https://doi.org/10.1016/s0896-6273(00)80391-8 PMID: 9390513.

32. Emerson MM, Surzenko N, Goetz JJ, Trimarchi J, Cepko CL. Otx2 and Onecut1 promote the fates of cone photoreceptors and horizontal cells and repress rod photoreceptors. Developmental cell. 2013; 26(1):59–72. Epub 2013/07/23. https://doi.org/10.1016/j.devcel.2013.06.005 PMID: 23867227; PubMed Central PMCID: PMC3819454.

33. Koike C, Nishida A, Ueno S, Saito H, Sanuki R, Sato S, et al. Functional roles of Otx2 transcription factor in postnatal mouse retinal development. Molecular and cellular biology. 2007; 27(23):8318–29. Epub 2007/10/03. https://doi.org/10.1128/MCB.01209-07 PMID: 17908793; PubMed Central PMCID: PMC2169187.

34. Nishida A, Furukawa A, Koike C, Tano Y, Aizawa S, Matsuo I, et al. Otx2 homeobox gene controls retinal photoreceptor cell fate and pineal gland development. Nat Neurosci. 2003; 6(12):1255–63. Epub 2003/11/20. https://doi.org/10.1038/nn1155 PMID: 14625556.

35. Dhanesh SB, Subashini C, James J. Hes1: the maestro in neurogenesis. Cell Mol Life Sci. 2016; 73(21):4019–42. Epub 2016/05/29. https://doi.org/10.1007/s00018-016-2277-z PMID: 27233500.

36. Imayoshi I, Kageyama R. Oscillatory control of bHLH factors in neural progenitors. Trends Neurosci. 2014; 37(10):531–8. Epub 2014/08/26. https://doi.org/10.1016/j.tins.2014.07.006 PMID: 25149265.

37. Kageyama R, Ohtsuka T, Kobayashi T. The Hes gene family: repressors and oscillators that orchestrate embryogenesis. Development. 2007; 134(7):1243–51. https://doi.org/10.1242/dev.000786 PMID: 17329370.

38. Liu ZH, Dai XM, Du B. Hes1: a key role in stemness, metastasis and multidrug resistance. Cancer Biol Ther. 2015; 16(3):353–9. Epub 2015/03/18. https://doi.org/10.1080/15384047.2015.1016662 PMID: 25781910; PubMed Central PMCID: PMC4622741.

39. Harima Y, Imayoshi I, Shimojo H, Kobayashi T, Kageyama R. The roles and mechanism of ultradian oscillatory expression of the mouse Hes genes. Semin Cell Dev Biol. 2014; 34:85–90. Epub 2014/05/29. https://doi.org/10.1016/j.semcdb.2014.04.038 PMID: 24865153.

40. Imayoshi I, Isomura A, Harima Y, Kawaguchi K, Kori H, Miyachi H, et al. Oscillatory control of factors determining multipotency and fate in mouse neural progenitors. Science. 2013; 342(6163):1203–8. Epub 2013/11/02. https://doi.org/10.1126/science.1242366 PMID: 24179156.

41. Manning CS, Biga V, Boyd J, Kursawe J, Ymisson B, Spiller DG, et al. Quantitative single-cell live imaging links HES5 dynamics with cell-state and fate in murine neurogenesis. Nature Communications. 2019; 10(1). https://doi.org/10.1038/s41467-019-10734-8 PMID: 31249377

42. Tomita K, Ishibashi M, Nakahara K, Ang S-L, Nakanishi S, Guillemot F, et al. Mammalian hairy and Enhancer of split homolog 1 regulates differentiation of retinal neurons and is essential for eye morphogenesis. Neuron. 1996; 16:723–34. https://doi.org/10.1016/s0896-6273(00)80093-8 PMID: 8607991

43. Hatakeyama J, Bessho Y, Katoh K, Ookawara S, Fujioka M, Guillemot F, et al. Hes genes regulate size, shape and histogenesis of the nervous system by control of the timing of neural stem cell differentiation. Development. 2004; 131(22):5539–50. https://doi.org/10.1242/dev.01436 PMID: 15496443.

44. Kageyama R, Shimojo H, Imayoshi I. Dynamic expression and roles of Hes factors in neural development. Cell Tissue Res. 2014. Epub 2014/05/23. https://doi.org/10.1007/s00441-014-1888-7 PMID: 24850276.

45. Karlsson C, Brantsing C, Kageyama R, Lindahl A. HES1 and HES5 are dispensable for cartilage and endochondral bone formation. Cells Tissues Organs. 2010; 192(1):17–27. Epub 2010/02/06. https://doi.org/10.1159/000280416 PMID: 20134146.

46. Kita A, Imayoshi I, Hojo M, Kitagawa M, Kokubu H, Ohsawa R, et al. Hes1 and Hes5 control the progenitor pool, intermediate lobe specification, and posterior lobe formation in the pituitary development. Mol Endocrinol. 2007; 21(6):1458–66. Epub 2007/04/12. https://doi.org/10.1210/me.2007-0039 PMID: 17426285.

47. Ohtsuka T, Ishibashi M, Gradwohl G, Nakanishi S, Guillemot F, Kageyama R. Hes1 and Hes5 as Notch effectors in mammalian neuronal differentiation. The EMBO Journal. 1999; 18(8):2196–207. https://doi.org/10.1093/emboj/18.8.2196 PMID: 10205173

48. Ohtsuka T, Sakamoto M, Guillemot F, Kageyama R. Roles of the basic helix-loop-helix genes Hes1 and Hes5 in expansion of neural stem cells of the developing brain. J Biol Chem. 2001; 276 (32):30467–74. Epub 2001/06/16. https://doi.org/10.1074/jbc.M102420200 PMID: 11399758.

49. Baek JH, Hatakeyama J, Sakamoto S, Ohtsuka T, Kageyama R. Persistent and high levels of Hes1 expression regulate boundary formation in the developing central nervous system. Development. 2006; 133(13):2467–76. https://doi.org/10.1242/dev.02403 PMID: 16728479.

50. Bosze B, Moon MS, Kageyama R, Brown NL. Simultaneous Requirements for Hes1 in Retinal Neurogenesis and Optic Cup-Stalk Boundary Maintenance. J Neurosci. 2020; 40(7):1501–13. Epub 2020/01/18. https://doi.org/10.1523/JNEUROSCI.2327-19.2020 PMID: 31949107; PubMed Central PMCID: PMC7044741.

51. Takatsuka K, Hatakeyama J, Bessho Y, Kageyama R. Roles of the bHLH gene Hes1 in retinal morphogenesis. Brain Res. 2004; 1004(1–2):148–55. https://doi.org/10.1016/j.brainres.2004.01.045 PMID: 15033430.

52. Wall DS, Mears AJ, McNeill B, Mazerolle C, Thurig S, Wang Y, et al. Progenitor cell proliferation in the retina is dependent on Notch-independent Sonic hedgehog/Hes1 activity. J Cell Biol. 2009; 184 (1):101–12. Epub 2009/01/07. https://doi.org/10.1083/jcb.200805155 PMID: 19124651.

53. Imayoshi I, Shimogori T, Ohtsuka T, Kageyama R. Hes genes and neurogenin regulate non-neural versus neural fate specification in the dorsal telencephalic midline. Development. 2008; 135 (15):2531–41. Epub 2008/06/27. https://doi.org/10.1242/dev.021535 PMID: 18579678.

54. Maillard I, Fang T, Pear WS. Regulation of lymphoid development, differentiation, and function by the Notch pathway. Annu Rev Immunol. 2005; 23:945–74. Epub 2005/03/18. https://doi.org/10.1146/annurev.immunol.23.021704.115747 PMID: 15771590.

55. Maillard I, Schwarz BA, Sambandam A, Fang T, Shestova O, Xu L, et al. Notch-dependent T-lineage commitment occurs at extrathymic sites following bone marrow transplantation. Blood. 2006; 107 (9):3511–9. Epub 2006/01/07. https://doi.org/10.1182/blood-2005-08-3454 PMID: 16397133; PubMed Central PMCID: PMC1895767.

56. Maillard I, Weng AP, Carpenter AC, Rodriguez CG, Sai H, Xu L, et al. Mastermind critically regulates Notch-mediated lymphoid cell fate decisions. Blood. 2004; 104(6):1696–702. Epub 2004/06/10. https://doi.org/10.1182/blood-2004-02-0514 PMID: 15187027.

57. Sambandam A, Maillard I, Zediak VP, Xu L, Gerstein RM, Aster JC, et al. Notch signaling controls the generation and differentiation of early T lineage progenitors. Nat Immunol. 2005; 6(7):663–70. Epub 2005/06/14. https://doi.org/10.1038/ni1216 PMID: 15951813.

58. Rowan S, Cepko CL. Genetic analysis of the homeodomain transcription factor Chx10 in the retina using a novel multifunctional BAC transgenic mouse reporter. Dev Biol. 2004; 271(2):388–402. Epub 2004/06/30. https://doi.org/10.1016/j.ydbio.2004.03.039 PMID: 15223342.

59. Lee HY, Wroblewski E, Philips GT, Stair CN, Conley K, Reedy M, et al. Multiple requirements for Hes 1 during early eye formation. Dev Biol. 2005; 284(2):464–78. https://doi.org/10.1016/j.ydbio.2005.06.010 PMID: 16038893.

60. Riesenberg AN, Conley KW, Le TT, Brown NL. Separate and coincident expression of Hes1 and Hes5 in the developing mouse eye. Dev Dyn. 2018; 247(1):212–21. Epub 2017/07/05. https://doi.org/10.1002/dvdy.24542 PMID: 28675662; PubMed Central PMCID: PMC5739946.

61. Hirata H, Tomita K, Bessho Y, Kageyama R. Hes1 and Hes3 regulate maintenance of the isthmic organizer and development of the mid/hindbrain. EMBO J. 2001; 20(16):4454–66. Epub 2001/08/14. https://doi.org/10.1093/emboj/20.16.4454 PMID: 11500373; PubMed Central PMCID: PMC125583.

62. Visel A, Thaller C, Eichele G. GenePaint.org: an atlas of gene expression patterns in the mouse embryo. Nucleic acids research. 2004; 32:D552–6 Available from: https://gp3.mpg.de/viewer/setInfo/MH1106/0. https://doi.org/10.1093/nar/gkh029 PMID: 14681479

63. Pak T, Yoo S, Miranda-Angulo AL, Wang H, Blackshaw S. Rax-CreERT2 knock-in mice: a tool for selective and conditional gene deletion in progenitor cells and radial glia of the retina and hypothalamus. PLoS One. 2014; 9(4):e90381. Epub 2014/04/05. https://doi.org/10.1371/journal.pone.0090381 PMID: 24699247; PubMed Central PMCID: PMC3974648.

64. Cau E, Gradwohl G, Casarosa S, Kageyama R, Guillemot F. Hes genes regulate sequential stages of neurogenesis in the olfactory epithelium. Development. 2000; 127(11):2323–32. https://doi.org/10.1242/dev.127.11.2323 PMID: 10804175.

65. Bosze B, Suarez-Navarro J, Soofi A, Lauderdale JD, Dressler GR, Brown NL. Multiple roles for Pax2 in the embryonic mouse eye. Dev Biol. 2021; 472:18–29. Epub 2021/01/12. https://doi.org/10.1016/j.ydbio.2020.12.020 PMID: 33428890; PubMed Central PMCID: PMC7956245.

66. Schwarz M, Cecconi F, Bernier G, Andrejewski N, Kammandel B, Wagner M, et al. Spatial specification of mammalian eye territories by reciprocal transcriptional repression of Pax2 and Pax6. Development. 2000; 127(20):4325–34. Epub 2000/09/27. https://doi.org/10.1242/dev.127.20.4325 PMID: 11003833.

67. Weinmaster G, Roberts VJ, Lemke G. A homolog of Drosophila Notch expressed during mammalian development. Development. 1991; 113(1):199–205. https://doi.org/10.1242/dev.113.1.199 PMID: 1764995.

68. Damiani D, Alexander JJ, O'Rourke JR, McManus M, Jadhav AP, Cepko CL, et al. Dicer inactivation leads to progressive functional and structural degeneration of the mouse retina. J Neurosci. 2008; 28(19):4878–87. Epub 2008/05/09. https://doi.org/10.1523/JNEUROSCI.0828-08.2008 PMID: 18463241; PubMed Central PMCID: PMC3325486.

69. Collinson JM, Quinn JC, Hill RE, West JD. The roles of Pax6 in the cornea, retina, and olfactory epithelium of the developing mouse embryo. Dev Biol. 2003; 255(2):303–12. Epub 2003/03/22. https://doi.org/10.1016/s0012-1606(02)00095-7 PMID: 12648492.

70. Sigulinsky CL, German ML, Leung AM, Clark AM, Yun S, Levine EM. Genetic chimeras reveal the autonomy requirements for Vsx2 in embryonic retinal progenitor cells. Neural Development. 2015; 10(1). https://doi.org/10.1186/s13064-015-0039-5 PMID: 25927996

71. Hatini V, Tao W, Lai E. Expression of winged helix genes, BF-1 and BF-2, define adjacent domains within the developing forebrain and retina. J Neurobiol. 1994; 25(10):1293–309. Epub 1994/10/01. https://doi.org/10.1002/neu.480251010 PMID: 7815060.

72. Huh S, Hatini V, Marcus RC, Li SC, Lai E. Dorsal-ventral patterning defects in the eye of BF-1-deficient mice associated with a restricted loss of shh expression. Dev Biol. 1999; 211(1):53–63. Epub 1999/06/22. https://doi.org/10.1006/dbio.1999.9303 PMID: 10373304.

73. Hiscock TW, Miesfeld JB, Mosaliganti KR, Link BA, Megason SG. Feedback between tissue packing and neurogenesis in the zebrafish neural tube. Development. 2018; 145(9). Epub 2018/04/22. https://doi.org/10.1242/dev.157040 PMID: 29678815; PubMed Central PMCID: PMC5992593.

74. Norden C, Young S, Link BA, Harris WA. Actomyosin is the main driver of interkinetic nuclear migration in the retina. Cell. 2009; 138(6):1195–208. Epub 2009/09/22. https://doi.org/10.1016/j.cell.2009.06.032 PMID: 19766571; PubMed Central PMCID: PMC2791877.

75. Hemesath TJ, Steingrimsson E, McGill G, Hansen MJ, Vaught J, Hodgkinson CA, et al. microphthalmia, a critical factor in melanocyte development, defines a discrete transcription factor family. Genes Dev. 1994; 8(22):2770–80. Epub 1994/11/15. https://doi.org/10.1101/gad.8.22.2770 PMID: 7958932.

76. Hodgkinson CA, Moore KJ, Nakayama A, Steingrimsson E, Copeland NG, Jenkins NA, et al. Mutations at the mouse microphthalmia locus are associated with defects in a gene encoding a novel basic-helix-loop-helix-zipper protein. Cell. 1993; 74(2):395–404. Epub 1993/07/30. https://doi.org/10.1016/0092-8674(93)90429-t PMID: 8343963.

77. Liu IS, Chen JD, Ploder L, Vidgen D, van der Kooy D, Kalnins VI, et al. Developmental expression of a novel murine homeobox gene (Chx10): evidence for roles in determination of the neuroretina and inner nuclear layer. Neuron. 1994; 13(2):377–93. Epub 1994/08/01. https://doi.org/10.1016/0896-6273(94)90354-9 PMID: 7914735.

78. Mastick GS, Andrews GL. Pax6 regulates the identity of embryonic diencephalic neurons. Molecular and cellular neurosciences. 2001; 17(1):190–207. Epub 2001/02/13. https://doi.org/10.1006/mcne.2000.0924 PMID: 11161479.

79. Kameda Y, Saitoh T, Fujimura T. Hes1 regulates the number and anterior-posterior patterning of mesencephalic dopaminergic neurons at the mid/hindbrain boundary (isthmus). Dev Biol. 2011; 358(1):91–101. Epub 2011/07/30. https://doi.org/10.1016/j.ydbio.2011.07.016 PMID: 21798254.

80. Maeda Y, Isomura A, Masaki T, Kageyama R. Differential cell-cycle control by oscillatory versus sustained Hes1 expression via p21. Cell reports. 2023; 42(5):112520. Epub 2023/05/18. https://doi.org/10.1016/j.celrep.2023.112520 PMID: 37200191.

81. Glickstein SB, Alexander S, Ross ME. Differences in cyclin D2 and D1 protein expression distinguish forebrain progenitor subsets. Cerebral cortex (New York, NY: 1991). 2007; 17(3):632–42. Epub 2006/04/22. https://doi.org/10.1093/cercor/bhk008 PMID: 16627858.

82. Saravanamuthu SS, Le TT, Gao CY, Cojocaru RI, Pandiyan P, Liu C, et al. Conditional ablation of the Notch2 receptor in the ocular lens. Dev Biol. 2012; 362(2):219–29. Epub 2011/12/17. https://doi.org/10.1016/j.ydbio.2011.11.011 PMID: 22173065; PubMed Central PMCID: PMC3265577.

83. Rowan S, Conley KW, Le TT, Donner AL, Maas RL, Brown NL. Notch signaling regulates growth and differentiation in the mammalian lens. Dev Biol. 2008; 321(1):111–22. Epub 2008/07/01. https://doi.org/10.1016/j.ydbio.2008.06.002 [pii] PMID: 18588871; PubMed Central PMCID: PMC2593917.

84. Wang Q, Marcucci F, Cerullo I, Mason C. Ipsilateral and Contralateral Retinal Ganglion Cells Express Distinct Genes during Decussation at the Optic Chiasm. eNeuro. 2016; 3(6). Epub 2016/12/14. https://doi.org/10.1523/ENEURO.0169-16.2016 PMID: 27957530; PubMed Central PMCID: PMC5136615.

85. Bertuzzi S, Hindges R, Mui SH, O'Leary DD, Lemke G. The homeodomain protein vax1 is required for axon guidance and major tract formation in the developing forebrain. Genes Dev. 1999; 13(23):3092–105. Epub 1999/12/22. https://doi.org/10.1101/gad.13.23.3092 PMID: 10601035; PubMed Central PMCID: PMC317177.

86. Hallonet M, Hollemann T, Wehr R, Jenkins NA, Copeland NG, Pieler T, et al. Vax1 is a novel homeobox-containing gene expressed in the developing anterior ventral forebrain. Development. 1998; 125(14):2599–610. Epub 1998/06/24. https://doi.org/10.1242/dev.125.14.2599 PMID: 9636075.

87. Morcillo J, Martinez-Morales JR, Trousse F, Fermin Y, Sowden JC, Bovolenta P. Proper patterning of the optic fissure requires the sequential activity of BMP7 and SHH. Development. 2006; 133(16):3179–90. Epub 2006/07/21. https://doi.org/10.1242/dev.02493 PMID: 16854970.

88. Kaufman ML, Goodson NB, Park KU, Schwanke M, Office E, Schneider SR, et al. Initiation of Otx2 expression in the developing mouse retina requires a unique enhancer and either Ascl1 or Neurog2 activity. Development. 2021; 148(12). Epub 2021/06/19. https://doi.org/10.1242/dev.199399 PMID: 34143204; PubMed Central PMCID: PMC8254865.

89. Kwong JM, Caprioli J, Piri N. RNA binding protein with multiple splicing: a new marker for retinal ganglion cells. Investigative ophthalmology & visual science. 2010; 51(2):1052–8. Epub 2009/09/10. https://doi.org/10.1167/iovs.09-4098 PMID: 19737887; PubMed Central PMCID: PMC3979483.

90. Rodriguez AR, de Sevilla Müller LP, Brecha NC. The RNA binding protein RBPMS is a selective marker of ganglion cells in the mammalian retina. The Journal of comparative neurology. 2014; 522(6):1411–43. Epub 2013/12/10. https://doi.org/10.1002/cne.23521 PMID: 24318667; PubMed Central PMCID: PMC3959221.

91. Chen S, Wang QL, Nie Z, Sun H, Lennon G, Copeland NG, et al. Crx, a novel Otx-like paired-homeodomain protein, binds to and transactivates photoreceptor cell-specific genes. Neuron. 1997; 19(5):1017–30. Epub 1997/12/09. https://doi.org/10.1016/s0896-6273(00)80394-3 PMID: 9390516.

92. Chen S, Wang QL, Xu S, Liu I, Li LY, Wang Y, et al. Functional analysis of cone-rod homeobox (CRX) mutations associated with retinal dystrophy. Hum Mol Genet. 2002; 11(8):873–84. https://doi.org/10.1093/hmg/11.8.873 PMID: 11971869.

93. Freund CL, Gregory-Evans CY, Furukawa T, Papaioannou M, Looser J, Ploder L, et al. Cone-rod dystrophy due to mutations in a novel photoreceptor-specific homeobox gene (CRX) essential for maintenance of the photoreceptor. Cell. 1997; 91(4):543–53. https://doi.org/10.1016/s0092-8674(00)80440-7 PMID: 9390563

94. Furukawa T, Morrow EM, Cepko CL. Crx, a novel otx-like homeobox gene, shows photoreceptor specific expression and regulates photoreceptor differentiation. Cell. 1997b; 91:531–41. https://doi.org/10.1016/s0092-8674(00)80439-0 PMID: 9390562

95. Prasov L, Glaser T. Pushing the envelope of retinal ganglion cell genesis: context dependent function of Math5 (Atoh7). Dev Biol. 2012; 368(2):214–30. Epub 2012/05/23. https://doi.org/10.1016/j.ydbio.2012.05.005 PMID: 22609278; PubMed Central PMCID: PMC3402631.

96. Cheng H, Khanna H, Oh EC, Hicks D, Mitton KP, Swaroop A. Photoreceptor-specific nuclear receptor NR2E3 functions as a transcriptional activator in rod photoreceptors. Hum Mol Genet. 2004; 13(15):1563–75. Epub 2004/06/11. https://doi.org/10.1093/hmg/ddh173 [pii]. PMID: 15190009.

97. Corbo JC, Cepko CL. A hybrid photoreceptor expressing both rod and cone genes in a mouse model of enhanced S-cone syndrome. PLoS Genet. 2005; 1(2):e11. https://doi.org/10.1371/journal.pgen.0010011 PMID: 16110338.

98. Ng L, Hurley JB, Dierks B, Srinivas M, Salto C, Vennstrom B, et al. A thyroid hormone receptor that is required for the development of green cone photoreceptors. Nat Genet. 2001; 27(1):94–8. https://doi.org/10.1038/83829 PMID: 11138006.

99. Ng L, Ma M, Curran T, Forrest D. Developmental expression of thyroid hormone receptor beta2 protein in cone photoreceptors in the mouse. Neuroreport. 2009; 20(6):627–31. Epub 2009/03/14. https://doi.org/10.1097/WNR.0b013e32832a2c63 PMID: 19282790.

100. Javed A, Santos-França PL, Mattar P, Cui A, Kassem F, Cayouette M. Ikaros family proteins redundantly regulate temporal patterning in the developing mouse retina. Development. 2023; 150(2). Epub 2022/12/21. https://doi.org/10.1242/dev.200436 PMID: 36537580.

101. Freund CL, Wang QL, Chen S, Muskat BL, Wiles CD, Sheffield VC, et al. *De novo* mutations in the CRX homeobox gene associated with Leber congenital amaurosis. Nat Genet. 1998; 18:311–2.

102. Brzezinski IV JAt Lamba DA, Reh TA. Blimp1 controls photoreceptor versus bipolar cell fate choice during retinal development. Development. 2010; 137(4):619–29. Epub 2010/01/30. 137/4/619 [pii] https://doi.org/10.1242/dev.043968 PMID: 20110327; PubMed Central PMCID: PMC2827615.

103. Katoh K, Omori Y, Onishi A, Sato S, Kondo M, Furukawa T. Blimp1 suppresses Chx10 expression in differentiating retinal photoreceptor precursors to ensure proper photoreceptor development. J Neurosci. 2010; 30(19):6515–26. Epub 2010/05/14. https://doi.org/10.1523/JNEUROSCI.0771-10.2010 PMID: 20463215; PubMed Central PMCID: PMC6632581.

104. Jin K, Xiang M. Transcription factor Ptf1a in development, diseases and reprogramming. Cellular and Molecular Life Sciences. 2018; 76(5):921–40. https://doi.org/10.1007/s00018-018-2972-z PMID: 30470852

105. Fujitani Y, Fujitani S, Luo H, Qiu F, Burlison J, Long Q, et al. Ptf1a determines horizontal and amacrine cell fates during mouse retinal development. Development. 2006; 133(22):4439–50. https://doi.org/10.1242/dev.02598 PMID: 17075007

106. Jin K, Jiang H, Xiao D, Zou M, Zhu J, Xiang M. Tfap2a and 2b act downstream of Ptf1a to promote amacrine cell differentiation during retinogenesis. Molecular brain. 2015; 8:28. Epub 2015/05/15. https://doi.org/10.1186/s13041-015-0118-x PMID: 25966682; PubMed Central PMCID: PMC4429372.

107. Nakhai H, Sel S, Favor J, Mendoza-Torres L, Paulsen F, Duncker GI, et al. Ptf1a is essential for the differentiation of GABAergic and glycinergic amacrine cells and horizontal cells in the mouse retina. Development. 2007; 134(6):1151–60. Epub 2007/02/16. https://doi.org/10.1242/dev.02781 PMID: 17301087.

108. Hojo M, Ohtsuka T, Hashimoto N, Gradwohl G, Guillemot F, Kageyama R. Glial cell fate specification modulated by the bHLH gene Hes5 in mouse retina. Development. 2000; 127(12):2515–22. https://doi.org/10.1242/dev.127.12.2515 PMID: 10821751.

109. Hong CS, Saint-Jeannet JP. The b-HLH transcription factor Hes3 participates in neural plate border formation by interfering with Wnt/β-catenin signaling. Dev Biol. 2018; 442(1):162–72. Epub 2018/07/18. https://doi.org/10.1016/j.ydbio.2018.07.011 PMID: 30016640; PubMed Central PMCID: PMC6138557.

110. Poser SW, Park DM, Androutsellis-Theotokis A. The STAT3-Ser/Hes3 signaling axis in cancer. Frontiers in bioscience (Landmark edition). 2014; 19(4):718–26. Epub 2014/01/07. https://doi.org/10.2741/4238 PMID: 24389215.

111. Harada H, Sato T, Nakamura H. Fgf8 signaling for development of the midbrain and hindbrain. Development, growth & differentiation. 2016; 58(5):437–45. Epub 2016/06/09. https://doi.org/10.1111/dgd.12293 PMID: 27273073.

112. Dakubo GD, Wallace VA. Hedgehogs and retinal ganglion cells: organizers of the mammalian retina. Neuroreport. 2004; 15(3):479–82. https://doi.org/10.1097/00001756-200403010-00019 PMID: 15094507.

113. Martinez-Morales J-R, Cavodeassi F, Bovolenta P. Coordinated Morphogenetic Mechanisms Shape the Vertebrate Eye. Frontiers in Neuroscience. 2017;11. https://doi.org/10.3389/fnins.2017.00721 PMID: 29326547

114. Giger FA, Houart C. The Birth of the Eye Vesicle: When Fate Decision Equals Morphogenesis. Front Neurosci. 2018; 12:87. Epub 2018/03/09. https://doi.org/10.3389/fnins.2018.00087 PMID: 29515359; PubMed Central PMCID: PMC5826324.

115. Kowalchuk AM, Maurer KA, Shoja-Taheri F, Brown NL. Requirements for Neurogenin2 during mouse postnatal retinal neurogenesis. Dev Biol. 2018; 442(2):220–35. Epub 2018/07/27. https://doi.org/10.1016/j.ydbio.2018.07.020 PMID: 30048641; PubMed Central PMCID: PMC6143394.

116. Mumm JS, Kopan R. Notch signaling: from the outside in. Dev Biol. 2000; 228(2):151–65. https://doi.org/10.1006/dbio.2000.9960 PMID: 11112321.

117. Kumar V, Vashishta M, Kong L, Wu X, Lu JJ, Guha C, et al. The Role of Notch, Hedgehog, and Wnt Signaling Pathways in the Resistance of Tumors to Anticancer Therapies. Front Cell Dev Biol. 2021; 9:650772. Epub 2021/05/11. https://doi.org/10.3389/fcell.2021.650772 PMID: 33968932; PubMed Central PMCID: PMC8100510.

118. Quaranta R, Pelullo M, Zema S, Nardozza F, Checquolo S, Lauer DM, et al. Maml1 acts cooperatively with Gli proteins to regulate sonic hedgehog signaling pathway. Cell Death & Disease. 2017; 8(7): e2942–e. https://doi.org/10.1038/cddis.2017.326 PMID: 28726779

119. Ahnfelt-Ronne J, Jorgensen MC, Klinck R, Jensen JN, Fuchtbauer EM, Deering T, et al. Ptf1a-mediated control of Dll1 reveals an alternative to the lateral inhibition mechanism. Development. 2012; 139 (1):33–45. Epub 2011/11/19. https://doi.org/10.1242/dev.071761 PMID: 22096075; PubMed Central PMCID: PMC3231770.

120. Beres TM, Masui T, Swift GH, Shi L, Henke RM, MacDonald RJ. PTF1 is an organ-specific and Notch-independent basic helix-loop-helix complex containing the mammalian Suppressor of Hairless (RBP-J) or its paralogue, RBP-L. Molecular and cellular biology. 2006; 26(1):117–30. Epub 2005/12/16. https://doi.org/10.1128/MCB.26.1.117-130.2006 PMID: 16354684; PubMed Central PMCID: PMC1317634.

121. Miesfeld JB, Moon MS, Riesenberg AN, Contreras AN, Kovall RA, Brown NL. Rbpj direct regulation of Atoh7 transcription in the embryonic mouse retina. Sci Rep. 2018; 8(1):10195. Epub 2018/07/07. https://doi.org/10.1038/s41598-018-28420-y PMID: 29977079; PubMed Central PMCID: PMC6033939.

122. Gong S, Zheng C, Doughty ML, Losos K, Didkovsky N, Schambra UB, et al. A gene expression atlas of the central nervous system based on bacterial artificial chromosomes. Nature. 2003; 425 (6961):917–25. Epub 2003/10/31. https://doi.org/10.1038/nature02033 PMID: 14586460.

123. Soofi A, Levitan I, Dressler GR. Two novel EGFP insertion alleles reveal unique aspects of Pax2 function in embryonic and adult kidneys. Dev Biol. 2012; 365(1):241–50. Epub 2012/03/14. https://doi.org/10.1016/j.ydbio.2012.02.032 PMID: 22410172; PubMed Central PMCID: PMC3322280.

124. Scholpp S, Lohs C, Brand M. Engrailed and Fgf8 act synergistically to maintain the boundary between diencephalon and mesencephalon. Development. 2003; 130(20):4881–93. Epub 2003/08/15. https://doi.org/10.1242/dev.00683 PMID: 12917294.

125. Schindelin J, Arganda-Carreras I, Frise E, Kaynig V, Longair M, Pietzsch T, et al. Fiji: an open-source platform for biological-image analysis. Nature methods. 2012; 9(7):676–82. Epub 2012/06/30. https://doi.org/10.1038/nmeth.2019 PMID: 22743772; PubMed Central PMCID: PMC3855844.